SISSA - SCUOLA
INTERNAZIONALE
SUPERIORE
DI STUDI AVANZATI
TRIESTE
Strada Costiera 11

ISAS - INTERNATIONAL SCHOOL
FOR ADVANCED STUDIES

Looking Beyond the Standard Model in Flavour Violating Neutrino Physics and in Ordinary–Exotic Fermion Mixing

Thesis submitted for the degree of
"Doctor Philosophiæ"

CANDIDATE
Daniele Tommasini

SUPERVISOR
Antonio Masiero

October 1991

TRIESTE

Contents

Overview

Almost all the present accelerator data are consistent with the Glashow–Weinberg–Salam 'Standard Model' (SM) of electroweak interactions. One exception is given by tau lepton decay measurements, but even in this case the disagreement is not dramatic. The minimal SM is now tested at the quantum (1–loop) level in several precise experiments. There are some strong, but still controversial, evidences of a mixing of the electron neutrino with a 17KeV neutrino. Important missing points are the top–quark and the Higgs–boson, which have not yet been found and are predicted to exist by the model. There is the hope that at least the top will be produced in the next few years. This would allow to reduce the uncertanties, that arise from the lack of knowledge of the top mass, that affect the theoretical predictions of the SM, so that the large amount of precise experiments will be more effective to test the SM itself, and eventually to indicate signals of new physics.

Then, why look for new physics while waiting for the discovery of top-quark and Higgs boson? There are two main reasons for such an effort.

First, the SM is not completely satisfactory for several theoretical reasons. It has a lot of free parameters, the hierarchy of fermion masses is introduced by hand, and the mechanism of spontaneous breaking of the gauge symmetry suffers a serious naturalness 'hierarchy' problem. All the above difficulties are related to the Higgs sector of the model, introduced to ensure the renormalizability of the theory, but for which there is no experimental evidence yet. Furthermore, the SM does not achieve a complete unification of the known interactions, nor describe gravity. So, it is hard to believe that it is the final theory of everything.

Second, solar neutrino observations and possibly some astrophysical evidences (Dark Matter, ionization of interstellar matter) require non standard physics, as neutrino masses and oscillations and/or neutrino magnetic moments, and/or some non standard leptonic flavour changing mechanism.

For these reasons, it is of interest to study non–standard physics, with two different aims. First, to constrain the possible extensions of the SM, which solve some of its theoretical drawbacks, by analyzing the effects of the new physics on the several precise experiments available. Second, to study the possibilities to explain solar neutrino and astrophysical observations in the currently viable extensions of the SM. In this thesis, we have examined some aspects of both these approaches.

In the first chapter, we study the neutrino properties in the presence of non–standard interactions violating the leptonic numbers. We will consider in particular some Flavour Changing Neutral Current (FCNC) effects occurring in supersymmetric models, which predict new scalars interacting with the known matter.

In the remaining three chapters, we will present the available precise experimental data, including the recent LEP results, and use all of them to constrain general extensions of the SM where new (heavy) fermions, that could mix the known leptons and quarks, are introduced.

Chapter 1

Leptonic Numbers Violation in Supersymmetric Theories and Neutrino Physics

Lepton (L) and Baryon (B) numbers are known to be conserved up to the present experimental accuracies. Their conservation follows automatically from gauge invariance and particle content in the Standard Model (SM) of electro–weak interactions, which succesfully describes the experimental data up to the 100 GeV scale. In the minimal SM, with no right handed neutrino, also the single family lepton numbers, L_e, L_μ, L_τ, are conserved. This means that processes like $\mu \to e\gamma$, neutrino masses, oscillations and decays, are forbidden, consistently with their experimental unobservation.

There are nevertheless reasons to expect that the single lepton numbers L_e, L_μ, L_τ, and possibly the total B and L numbers, are not exact symmetries of Nature. Solar neutrino counting (and possibly few other astrophysical observations) seem to require at least L_e non–conservation. From a theoretical point of view, the SM is not completely satisfactory, in spite of its successes, and in most of its extensions L and B conservations are not automatic.

Neutrino masses and oscillations can be accomodated in the SM by the simple addition of the right handed neutrinos. This could be sufficient for the explanation of the deficit in the observation of solar neutrinos, through the MSW effect. But this almost minimal SM is still unsatisfactory for several theoretical reasons. It has a large number of parameters and it does not really unificate strong, electromagnetic and weak interactions; it does not *explain* masses and family replica; it does not describe the gravitational force. Furthermore, it is affected by the 'Hierarchy Problem': the electroweak scale ~ 100 GeV can not be naturally so many orders of magnitude smaller than the scale of a possible unification or than the Planck scale of Quantum Gravity.

Several possibilities of new physics have been proposed to solve the hierarchy problem. Amoung these attempts, Supersymmetric Theories (SUSY) deserve particular attention since they allow also to quantize gravity in a very elegant way (supergravity theories). Furthermore, Supersymmetric Grand Unified Theories (SGUT) predict a value of the weak mixing angle which is consistent with the recent and very accurate LEP result. Finally, even in the simplest supersymmetric extension of the SM with minimal particle content gauge invariance do not prevent explicit lepton number violation in the lagrangian.

In fact, many of the phenomenological consequences of SUSY theories with explicit L or B violation have already been studied in detail [1]. In this chapter we focus on the phenomenological aspects of these theories concerning the neutrino magnetic moments and decays.

In section 1 we introduce the formalism of the supersymmetric models which show interesting possibilities for lepton and lepton–flavor violation. We will briefly present the Supersymmetric Standard Model (SSM), both in the case of minimal and non–minimal supersymmetry soft–breaking sectors; then we will consider the simple generalization of the model allowing interactions which break B or L (L_i).

In section 2 we show that in these supersymmetric theories the lepton number violating couplings naturally give rise to significant neutrino magnetic moments at one loop. In the case of the Minimal SSM (MSSM) with explicit lepton number violation the transition magnetic moment $\mu_{\nu_e \nu_\mu}$ can be as large as $10^{-13}\mu_B$ ($\mu_B =$ Bohr magneton) [2], not far from the Barbieri–Fiorentini theoretical bound [3] discussed in the appendix. By requiring an $SU(2)_H$ horizontal symmetry of the Lagrangian in the Yukawa-less limit, $\mu_{\nu_e \nu_\mu}$ may be one order of magnitude larger. In this case the main naturalness constraint on the maximum $\mu_{\nu_e \nu_\mu}$ attainable is the electron mass value rather than the bound on the neutrino mass itself.

In section 3 we consider a scenario proposed by Sciama [4,5] where an 'heavy' neutrino ν_h of mass $m_{\nu_h} \sim 30$eV decays radiatively ($\nu_h \to \nu_l + \gamma$) in a much lighter neutrino ν_l with lifetime $\tau \sim 10^{23}s$. In this case, ν_h can provide the missing mass of the universe, and its radiative decay happens at the required rate to explain several astrophysical observations of the H_α emission lines and ionization of the HI clouds. We show in a model–independent way that the experimental limits on neutrino oscillations leave room for such 'Sciama' neutrinos only for neutrino magnetic moments close to the Barbieri–Fiorentini bound. We also show that in the Minimal SSM with broken lepton number this limit cannot be attained without getting too much neutrino oscillations, unless a cancellation mechanism for the off–diagonal term in the neutrino mass matrix is provided.

In section 4 we draw our conclusions and briefly overview some further developements on the subject.

1.1 The Supersymmetric Standard Model

1.1.1 The (minimal) particle content

The Supersymmetric Standard Model (SSM) [6] is an effective theory which is a candidate for the description of physics below the possible unification (or the Planck) energy scale. Supersymmetry requires that to each ordinary fermionic (bosonic) particle, a bosonic (fermionic) 'supersymmetric partner' is associated, which has the same quantum numbers (with the exception of the spin). To distinguish the two particles a further quantum number R_p called R–parity can be introduced, which is $+1$ for the ordinary particle, and -1 for its partner. For a particle of spin S,

$$R_p = (-1)^{3B+L+2S}. \tag{1.1}$$

The two partners can be arranged in a multiplet or superfield, which we will denote with the same symbol as the ordinary particle component, while the supersymmetric partner will be affected by a tilde. We then have the following superfields describing the 'light' particles:

the leptonic chiral superfields

$$L_i = \begin{pmatrix} \nu_i \\ e_i \end{pmatrix}, \qquad e_i^c,$$

(where $i = 1, 2, 3 = e, \mu, \tau$ is the generation index) whose fermionic components are the $SU(2)_L$ leptonic doublets and singlets respectively, and whose bosonic components are scalars called sleptons, $\tilde{L}_i = (\tilde{\nu}_i \quad \tilde{e}_i)^T$, $\tilde{e}^c_i$;

the quark chiral superfields

$$Q_i = \begin{pmatrix} u_i \\ d_i \end{pmatrix}, \qquad d^c_i,$$

$(i = 1, 2, 3)$ whose fermionic components are the left–handed doublets and singlets respectively, and whose bosonic components are the squark scalars $\tilde{Q}_i = (\tilde{u}_i \quad \tilde{d}_i)^T$, $\tilde{u}^c_i$ and $\tilde{d}^c_i$;

the two Higgs chiral superfields H_u, H_d, whose bosonic components are the ± 1 weak–hypercharge Higgs scalars, and whose fermionic components are the higgsinos $\tilde{H}_u$, $\tilde{H}_d$;

the vector–superfields with the gauge bosons as the spin 1 components and the gauginos as the spin $\frac{1}{2}$ components.

1.1.2 The R–parity conserving interactions

Given this particle content, the most general, $SU(3)_c \times SU(2)_L \times U(1)_Y$ gauge invariant superpotential is

$$f = f^{SSM} + f^{\not R}.$$

Here

$$f^{SSM} = h^u_{ij} Q_i H_u u^c_j + h^d_{ij} Q_i H_d d^c_j + h^e_{ij} L_i H_d e^c_j + \mu H_u H_d, \tag{1.2}$$

defines the SSM and is the R–parity conserving superpotential describing interactions involving an even number of supersymmetric partners. $f^{\not R}$ is the R–parity breaking superpotential, which will be discussed in the next subsection. We notice that the R–parity of a term of the superpotential is $R_p = (-1)^{3B+L}$, hence with the minimal particle content an interaction violates R_p if and only if it violates B or L.

Each term of the trilinear part of the superpotential f describes three Yukawa vertices, i.e. fermion-fermion-scalar, fermion-scalar-fermion, scalar-fermion-fermion. These three vertices have the same coupling constant as a consequence of the supersymmetry. The Yukawa couplings are related to the fermions mass matrices $m^q_{ij} = h^q_{ij} v_q$ $(q = u, d)$ and $m^e_{ij} = h^e_{ij} v_d$, where $v_q \equiv < H^0_q >$ are the vacuum expectation values of the neutral components of the two Higgs fields.

The scalar potential of the theory can be deduced by considering the function $f(\phi)$ of the set of scalar fields $\phi = \{\phi_a\}$, obtained by taking the scalar components of the fields in the formal expression for f,

$$V = \sum_{a=all\ scalars} \left| \frac{\partial f(\phi)}{\partial \phi_a} \right|^2 \tag{1.3}$$

This potential does not break neither supersymmetry, nor $SU(2)_L \times U(1)_Y$ gauge invariance. In the currently viable supergravity–induced SSM [6], both the gauge symmetry and the supersymmetry breaking arise from an additional contribution V_{soft} to the scalar potential, which breaks supersymmetry since it cannot be deduced from a superpotential. The 'soft–breaking' potential V_{soft} is bi– and tri– linear in the scalar fields, thus describing super–renormalizable interactions, which do not spoil the property of cancellation between fermion and boson loops in UV divergences that is necessary e.g. to overcome the hierarchy problem.

The general for of V_{soft} is

$$V_{soft}^{SSM} = \sum_{a=all\ scalars} m_a^2|\phi_a|^2 + m(\tilde{h}_{ij}^u \tilde{Q}_i H_u \tilde{u}_j^c + \tilde{h}_{ij}^d \tilde{Q}_i H_d \tilde{d}_j^c + \tilde{h}_{ij}^e \tilde{L}_i H_d \tilde{e}_j^c + \tilde{\mu} H_u H_d + h.c.)$$

The mass parameters m and m_a appearing in V_{soft}^{SSM} set the scale of both the global SUSY, and electroweak gauge symmetry, breakings. Their values are typically of the order of few 100 GeV's, with the experimental constraints $m_{\tilde{l}} \gtrsim 50$GeV and $m_{\tilde{q}} \gtrsim 100$GeV. The couplings $\tilde{h}$, $\tilde{\mu}$ in general are not known; their form can be specified if it is assumed that V_{soft} arises from a supergravity theory with a flat Kähler metric. In this case, at the superhigh energies of the local SUSY breaking, we have

$$\tilde{h}_{ij}^{MSSM} = h_{ij}, \tag{1.4}$$

i.e. equal to the yukawa couplings of the superpotential. The couplings $\tilde{h}^{MSSM}$ define the so–called Minimal SSM (MSSM) [6]. At the 'low energy' scale (accelerator energies), eq. (1.4) is corrected by radiative corrections, and the additional contributions generate FCNC's [7]. The MSSM is also characterized by $m_a \sim m$ independent of a. The resulting high degeneracy of the scalars masses suppresses dangerous FCNC's: this is a very welcome feature of the MSSM! By the way, even in a more general SSM this degeneracy has to be mantained to great accuracy, otherwise too large FCNC's would be induced.

1.1.3 The R–parity breaking interactions

Due to the presence of the sleptons and squarks, in SUSY models new vertices can be written, which directly break L and/or B. Only the imposition of a discrete symmetry, R–parity, allows to get rid of these interactions, and keep stable the proton, as well as the Lightest Supersymmetric Particle (LSP).

The possible R–breaking superpotential is

$$f^{\not R} = f^{\Delta L \neq 0} + f^{\Delta B \neq 0}, \tag{1.5}$$

where

$$f^{\Delta L \neq 0} = \lambda_{ijk} L_i L_j e^c_k + \lambda'_{ijk} L_i Q_j d^c_k \tag{1.6}$$

breaks the lepton number, while $f^{\Delta B \neq 0} = \lambda'' u^c_i d^c_j d^c_k$ breaks the baryon number. R–parity would be violated also by LH_u, but this term can be rotated away through a redefinition of L and H_d.

The phenomenological limits on the λ and λ' parameters have been found in ref. [8] in the hypotesis that only the considered single coupling is non negligible. The typical bounds are

$$|\lambda|, |\lambda'| \lesssim 0.1 \frac{m_0}{100\mathrm{GeV}}$$

where m_0 is a squark or slepton mass. For the parameters λ_{12k} and λ'_{11k} the constraint is stronger by a factor 3 since they would affect charged current universality, while for λ'_{12k} and λ'_{131} it is $\sim 0.4 m_0/100\mathrm{GeV}$. These 'single' bounds are surprisingly weak, but when two or more couplings are simultaneously allowed to exist, their possible products are usually severely constrained since they would yeld rare processes. We will consider exemples in the next section. The particularly dangerous simultaneous presence of L and B violating couplings can be avoided by requiring the conservation of either B or L. In our thesis we are interested in L violation, so that we will assume that B is conserved.

1.2 Neutrino magnetic moment in SUSY with broken R–parity

The attention to a possible connection between the sizeable neutrino magnetic moment and R-parity breaking in supersymmetric theories has been drawn by Babu and Mohapatra [9]. Here give a complete analysis of the problem, in order to get the naturally attainable values of the neutrino magnetic moments in different versions of the theory [2]. Applying a naturalness criterion, i.e. barring accidental cancellations among possible different contributions to the neutrino or the charged fermion masses, we come to the following conclusions. In the MSSM with R-parity broken in the superpotential, one can have neutrino magnetic moments of order $\mu \simeq 10^{-13}\mu_B$ ($\mu_B = e/2m_e$ Bohr magneton). In this version of the theory, the main constraint on μ is set by the upper bound on the neutrino masses ($m_{\nu_e} \lesssim 10eV$ from laboratory experiments, $m_{\nu_\mu}, m_{\nu_\tau} \lesssim 100eV$ from cosmology). Although a value of $\mu \simeq 10^{-13}\mu_B$ is not close to the present laboratory bounds ($\mu \lesssim 10^{-10} - 10^{-9}\mu_B$ for the electron and muon neutrinos), it is far larger than the "Standard Model value" [10] of the neutrino magnetic moment $\mu/\mu_B \lesssim (10^{-19} - 10^{-18})(m_{\nu_e}/eV)$.[1] In other words, supersymmetric theories with L-breaking couplings naturally get close to the Barbieri–Fiorentini [3] theoretical bound on the neutrino magnetic moment, discussed in the appendix.

To obtain $\mu \simeq 10^{-13}\mu_B$ in the MSSM does not require any particular symmetric structure of the Lagrangian. If such a symmetry is implemented, which

[1] This value is obtained by considering the simple extension of the SM including the right handed neutrino and Dirac ν masses; μ_{ν_e} is then generated at 1–loop by W exchange.

requires departing from the MSSM although still remaining with minimal particle content, an order of magnitude can be gained, leading to $\mu \lesssim 10^{-12}\mu_B$. This upper bound is obtained by applying the same naturalness criterion as before. In this case, the main constraint comes from the electron mass (or the d-quark mass) rather than the neutrino mass itself.

1.2.1 $\mu_{\nu_e \nu_\mu}$ in the MSSM

The MSSM [6] with explicit R-parity breaking via L-violation is described by the superpotential (1.6). The couplings induced by this superpotential are the ones that give rise to the neutrino magnetic moments, as well as to the neutrino mass. In particular, Fig. 1 shows all the one loop diagrams, arising from the purely leptonic couplings in (1.6), that contribute to the ν_e-ν_μ magnetic moment $\mu_{\nu_e \nu_\mu}$ after insertion of a photon vertex on any internal line.

The diagrams of Fig. 1 (a),(b) are characterized by the fact that the couplings involved conserve the difference between the electron and muon lepton number $L_e - L_\mu$, whereas the diagrams of Fig. 1 (c),(d) respect L_τ. Analogous diagrams exist, originating from the couplings in (1.6) involving the quark fields, with the internal leptons (sleptons) replaced by quarks (squarks). In all of these diagrams, that contribute as well to the mass term $m_{\nu_e \nu_\mu}$ if no photon vertex is inserted, an helicity flip on the internal fermion line is necessary. As explicitly indicated, this also requires a mixing of the scalar leptons associated with the different chiralities, described by the scalar Lagrangian term $\Delta_{ij}\tilde{l}_i\tilde{l}^c_j$.

In a general softly broken supersymmetric lagrangian, the mixing square mass

FIGURE 1. Supersymmetric contributions to $m_{\nu_e \nu_\mu}$ and to $\mu_{\nu_e \nu_\mu}$, when a photon line is inserted on each internal line.

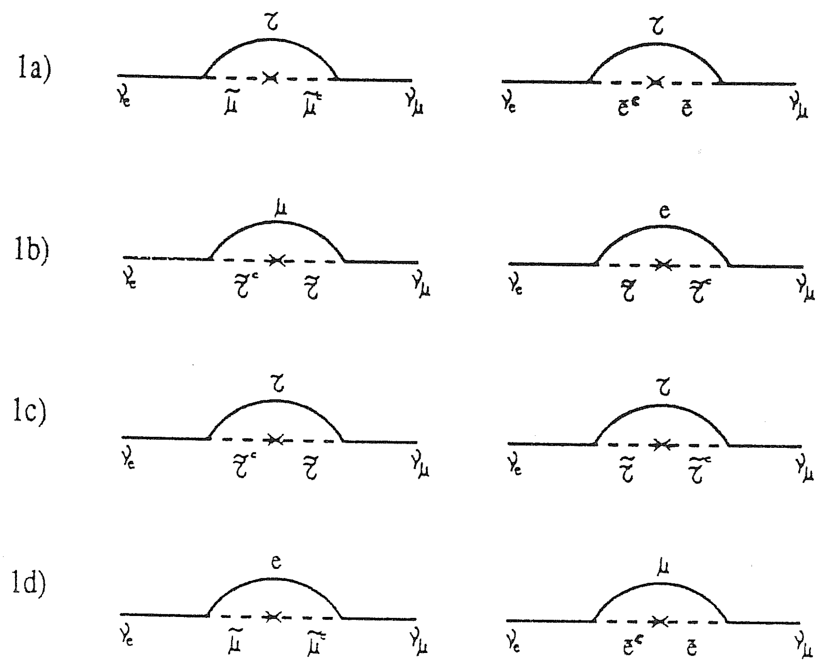

matrix Δ_{ij} receives two distinct contributions: one from the supersymmetric coupling (see (1.3) and (1.2)), $\mu(v_u/v_d)m_i\delta_{ij}$ in the physical basis for the leptons of mass m_i [6], and another from the soft supersymmetry-breaking term $\Delta_{ij}^{soft} = m\tilde{h}_{ij}v$ (where $v = v_u$ for the $\tilde{u}$ squark, $v = v_d$ for the $\tilde{d}$ and the sleptons $\tilde{e}$). For the purposes of the present discussion, the MSSM is characterized by the property that also Δ_{ij}^{soft} is diagonal in the physical leptons basis and proportional to the lepton masses (see (1.4)). One can therefore write

$$\Delta_{ij}^{\mathrm{MSSM}} = \tilde{m} m_i \delta_{ij} \tag{1.7}$$

where $\tilde{m}$ is typically of the order of the largest between m and $\mu v_u/v_d$. Furthermore, in the limit of vanishing lepton masses, the sleptons are degenerate at a mass m_0 (the splitting between left and right sleptons is irrelevant to the present discussion).

Notice that, in general, many more diagrams can be drawn, contributing to the diagonal neutrino mass terms, whereas the corresponding contributions to the diagonal neutrino magnetic moments vanish by Lorentz symmetry.

Any of the diagrams of Fig. 1 contribute to $m_{\nu_e\nu_\mu}$ and $\mu_{\nu_e\nu_\mu}$ (after insertion of the photon line) respectively as

$$\begin{aligned} \delta m_{\nu_e\nu_\mu} &\simeq \frac{\lambda_a\lambda_b}{16\pi^2} m_l \frac{\Delta}{m_0^2} \\ |\delta\mu_{\nu_e\nu_\mu}| &= \mu_B \frac{\lambda_a\lambda_b}{2\pi^2}\frac{m_e m_l}{m_0^2}\left(\log\left(\frac{m_0}{m_l}\right)-1\right)\frac{\Delta}{m_0^2} \end{aligned} \tag{1.8}$$

where m_l is the mass of the internal charged lepton, λ_a and λ_b are the appropriate couplings, and Δ is the required mixing term. Of course $m_l/m_0 \ll 1$ and we are also making an expansion in Δ/m_0^2. For any of the individual corresponding contributions in (1.8) we have

$$|\delta\mu_{\nu_e\nu_\mu}| = \mu_B \delta m_{\nu_e\nu_\mu} \frac{8m_e}{m_0^2}\left(\log\left(\frac{m_0}{m_l}\right)-1\right). \tag{1.9}$$

For each single product $\lambda_a\lambda_b$ there are two comparable graphs contributing to $\delta m_{\nu_e\nu_\mu}$ and to $|\delta\mu_{\nu_e\nu_\mu}|$. If we now require that each contribution to $\delta m_{\nu_e\nu_\mu}$ proportional to a fixed product $\lambda_a\lambda_b$ be less than $10eV$, we get a bound on the corresponding $|\delta\mu_{\nu_e\nu_\mu}|$ with a logarithmic dependence on the masses m_l of the lepton exchanged. Numerically

$$|\delta\mu_{\nu_e\nu_\mu}| \lesssim \mu_B \cdot (0.2 - 0.4)\cdot 10^{-13}\left(\frac{100GeV}{m_0}\right)^2, \tag{1.10}$$

where the coefficient depends on which pair of graphs one is considering. From the negative experimental searches of sleptons, m_0 can be as low as $50GeV$, implying

$$|\delta\mu_{\nu_e\nu_\mu}| \lesssim O(10^{-13}\mu_B). \tag{1.11}$$

This bound can be saturated if and when the bound on the neutrino mass is saturated. In turn, for any given pair of diagrams (with definite lepton-slepton pair exchange), using (1.7) for the scalar mixing, this only depends on the values of the L-violating couplings λ_a, λ_b. Effects associated with the individual presence of any of these couplings have been studied in the literature [8] and the corresponding bounds obtained. The simultaneous presence of a pair of couplings required by the mass or the magnetic moment diagrams generally leads to stronger limits. They are:

i) for the couplings relevant to the diagrams of Fig. 1 (d), from the $\mu \to 3e$ process

$$\lambda_{122}\lambda_{121} \lesssim 10^{-6}\left(\frac{m_0}{100GeV}\right)^2 \tag{1.12}$$

ii) from the $\mu \to e\gamma$ transition, for the couplings occurring in Fig. 1 (c)

$$\lambda_{233}\lambda_{133} \lesssim 10^{-5}\left(\frac{m_0}{100GeV}\right)^2 \tag{1.13}$$

Both these bounds are stronger than the products of the individual limits [8] and do not allow the saturation of (1.10) by the corresponding diagrams. On the other hand, no limit exists on the products $\lambda_{123}\lambda_{232}$ of the couplings entering the first ones of the diagrams of Fig. 1 (a),(b) stronger than the limit obtained requiring that this same contribution to $\delta m_{\nu_e\nu_\mu}$ be less than $10eV$, i.e.

$$\lambda_{123}\lambda_{232} \leq 4\cdot 10^{-4}\left(\frac{m_0}{\tilde{m}}\right)\left(\frac{m_0}{100GeV}\right). \tag{1.14}$$

To get this bound, the form (1.7) for the scalar mixing term has been assumed. As a consequence, the related diagrams may give contributions to the magnetic moments of order $10^{-13}\mu_B$.

We neglected in our discussion the contribution of the second two diagrams of Fig. 1 (a),(b) since it cannot saturate the bound (1.11). In fact, these diagrams, which in the MSSM of eq. (1.7) are proportional to the electron mass, are mostly limited by the product $\lambda_{123}\lambda_{131} < 4 \cdot 10^{-3}(m_0/100GeV)^2$ of the individual bounds [8] on the relevant couplings. This ensures that their contribution to $\delta m_{\nu_e\nu_\mu}$ be an order of magnitude smaller than $10eV$.

Analogous considerations can be made for the diagrams involving the quark and squarks exchanges. Some of them may indeed give contributions comparable to the largest terms involving leptons (sleptons) only ($\delta\mu \simeq O(10^{-13}\mu_B)$). However one must be careful about the effects induced by the Cabibbo-Kobayashi-Maskawa mixings which result into the breaking, together with the R-parity breaking couplings, of all the individual lepton numbers.

1.2.2 $\mu_{\nu_e\nu_\mu}$ in non–minimal SSM

We have seen that the MSSM may naturally give neutrino magnetic moments which far exceed the so-called "Standard Model value", without invoking any particular symmetry structure of the Lagrangian. This suggests to ask whether a suitable departure from the MSSM may lead to even bigger neutrino magnetic moments. The role of appropriate approximate symmetries of the Lagrangian in connection with the neutrino problem has been recently emphasized [9,11,12].

Along these lines we require that our Lagrangian, in the limit of vanishing Yukawa couplings, be symmetric under an $SU(2)_H$ horizontal symmetry acting on the first and the second generations. In connection with the neutrino magnetic moment, this same symmetry has already been invoked in a non supersymmetric context in ref. [12] and in the supersymmetric case in ref. [9]. In our view all of these models have problems with the $e-\mu$ mass splitting, which represents a violation of the $SU(2)_H$-symmetry. The description of the $e-\mu$ mass difference by explicit different Yukawa couplings in a non-supersymmetric context looks unnatural because of the quadratic divergences induced by loops in asymmetric renormalizable operators. On the other hand, and perhaps more seriously, the breaking of the $SU(2)_H$ symmetry by soft terms [9] may account for the $e-\mu$ mass difference generated by radiative corrections only by an unnatural fine tuning, if possible at all.

Here we assume [2,13] that the $SU(2)_H$ symmetry be respected in the Yukawa-less limit of the supersymmetric Lagrangian, including the soft breaking terms and the L-violating couplings, being just violated by the standard supersymmetric Yukawa couplings for the electron and the muon. For the consistency of the theory, we rely on the absence of quadratic divergences in supersymmetric theories. Small violations of the $SU(2)_H$ symmetry will also have to be present, for example, in the scalar mixing terms, but they will be controlled by the small Yukawa couplings and they will not be quadratically divergent. Departing from the MSSM, we will assume for these mixings terms

$$\Delta_{11} \simeq \Delta_{22} \gg |\Delta_{11} - \Delta_{22}| \simeq \tilde{m} m_\mu \tag{1.15}$$

Let us now reconsider the diagrams of Fig.1. The $SU(2)_H$ symmetry forbids the diagrams 1 (c),(d), since the individual couplings entering the diagrams violate the horizontal $SU(2)_H$. On the other hand, the allowed diagrams 1 (a),(b) in the exact $SU(2)_H$ limit contribute to the magnetic moment (after the photon insertion), which is an $SU(2)_H$ singlet term, but do not to the mass, which is a triplet. In practical terms, a cancellation takes place in the mass diagrams 1 (a),(b) between the electron (selectron) and the muon (smuon) diagram, whereas the related magnetic moment terms add coherently. This allows to evade the neutrino mass bound as the strongest restriction on the magnetic moment. With respect to the previous considerations in the MSSM, we offer a symmetry reason for a natural cancellation among different mass terms.

The cancellation is most efficient in the diagrams 1 (a), which are the interesting source of the sizeable magnetic moment. Their contribution to $m_{\nu_e\nu_\mu}$ is

$$\delta m_{\nu_e\nu_\mu} = \frac{\lambda_{123}\lambda_{232}}{16\pi^2} m_\tau \frac{\Delta_{22} - \Delta_{11}}{m_0^2} = \frac{\lambda_{123}\lambda_{232}}{16\pi^2} m_\tau m_\mu \frac{\tilde{m}}{m_0^2} \tag{1.16}$$

which is safe ($\delta m_{\nu_e\nu_\mu} < 10eV$), provided

$$\lambda_{123}\lambda_{232} < 9 \cdot 10^{-4} \left(\frac{m_0}{\tilde{m}}\right) \left(\frac{m_0}{100GeV}\right). \tag{1.17}$$

On the other hand, their contribution to $\mu_{\nu_e\nu_\mu}$ is sensitive to $\Delta_{22} \simeq \Delta_{11}$ and not to their difference. The constraint (1.17) is then not enough to bound $\mu_{\nu_e\nu_\mu}$. Rather it is the contribution to the electron mass shown in Fig. 2 that provides the main restriction. From this diagram, where a neutral gaugino is exchanged, we have

$$\delta m_e = \frac{e^2}{16\pi^2} \sum_i \left(V_{1i}^2 + \frac{1}{\sin^2\theta_W \cos^2\theta_W} V_{2i}^2 \right) F(m_i)\Delta_{11} \tag{1.18}$$

where θ_W is the weak mixing angle,

$$F(m) = \frac{m}{m^2 - m_0^2}\left[1 + \frac{2m^2}{m^2 - m_0^2}\log\left(\frac{m_0}{m}\right)\right] \tag{1.19}$$

and m_i is the i-th eigenvalue of the neutralino mass matrix, diagonalized by the matrix V_{ij} from the usual basis $\chi_N = (\tilde{\gamma}, \tilde{Z}, \tilde{h}_1, \tilde{h}_2)$. We are, of course, using the fact that only the gaugino couplings are relevant in Fig. 2 and not the couplings to the Higgsinos $\tilde{h}_{1,2}$. From (1.18) and (1.19), requiring $\delta m_e < 0.5MeV$, $m_{\chi_N} \gtrsim 20GeV$ and $m_0 \gtrsim 50GeV$, we infer

$$\Delta_{11} \lesssim 100GeV^2 \tag{1.20}$$

This bound can either be saturated for light gaugino masses m_i's or for heavy ones $m_i \lesssim 1TeV$.

FIGURE 2. Supersymmetric contribution to the electron mass.

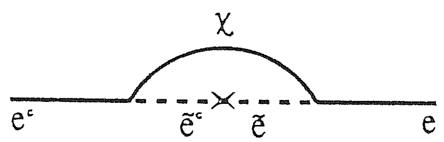

The same mass insertion as in Fig. 2 enters in the τ-neutrino mass diagram of Fig. 3 as well. However, requiring $\delta m_{\nu_\tau} < 100eV$ for consistency with cosmology and using $\Delta_{22} \simeq \Delta_{11} \lesssim 100GeV^2$ gives $\lambda_{232} \lesssim 0.05(m_0/100GeV)$, which is

FIGURE 3. Supersymmetric contribution to the tau–neutrino mass.

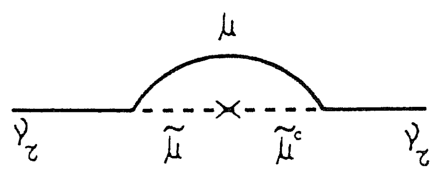

only slightly more restrictive than the limit $\lambda_{232} \lesssim 0.09(m_0/100GeV)$ from lepton universality [8] and does not prevent the saturation of the bound (1.17) even taking into account $\lambda_{123} \lesssim 0.04(m_0/100GeV)$ from charged current quark-lepton universality [8].

Putting all together, from the diagrams of Fig. 1 (a), we find, using eqs. (1.8), (1.17), (1.20)

$$\delta\mu_{\nu_e\nu_\mu} \lesssim O(10^{-12}\mu_B) \tag{1.21}$$

We think that this is the largest value one can obtain for the neutrino magnetic moment in a completely natural way in a supersymmetric theory with minimal particle content.

We have also considered, as in the MSSM cases, the possible contribution of the quark-squark diagrams with the $SU(2)_H$-symmetry implemented. In this case a strong constraint comes from the 1-loop contribution to the d-quark mass, involving the creation and annihilation of a gluino-sdown pair, analogous to the electron mass diagram of Fig 2. Also in view of the bounds on the squarks masses which are stronger than the corresponding ones for the sleptons, the value (1.21) cannot be attained by the quark-squark contributions.

1.3 Cosmologically interesting neutrino decay with flavour violation

Neutrinos from the early universe survive until today in large amounts, with average number density $\sim 115\text{cm}^{-3}$ for each ν species. Hence, if neutrinos are massive with $\sum m_{\nu_i} \simeq (10-100)$ eV, they provide a significant contribution to the energy density of the universe and may even account for the Dark Matter. If the heaviest neutrino ν_h is unstable, decaying radiatively into a lighter one ν_l through the process $\nu_h \to \nu_l + \gamma$, then the U.V. photons produced by this large amount of relic neutrinos can have important astrophysical implications. De Rújula and Glashow [14] suggested that these γ's could be searched in the U.V. background on the earth, and Mellot and Sciama [15] suggested that they could produce important ionization of interstellar matter. More recently, Sciama [4] has extended this proposal to explain the ionization of the HI regions in the galaxy, finding an agreement with the observations if the decay lifetime is $\tau \simeq 1.5 \cdot 10^{23} s$ and $m_{\nu_h} \simeq 28$ eV (for negligible m_{ν_l}).[2] Furthermore, this scenario implies some interesting predictions such as a value for the Hubble expansion rate of $H \simeq 55\text{km} \cdot s^{-1} Mpc^{-1}$ (for $\Omega \simeq 1$) [5], and seems to be compatible with the Tremaine-Gunn phase space constraint, which allows ν_h to provide the Dark Matter in galaxies [16].

[2] Actually, it is necessary that the photon energy E_γ satisfies $2E_\gamma = m_{\nu_h} - m^2_{\nu_l}/m_{\nu_h} = 27.7 \pm 0.5$ eV.

Some *ad hoc* models [17] have been proposed where these neutrino properties can be achieved, but they are not completely satisfactory from a theoretical and aesthetical point of view. Most of these models [17,11] extend the SM introducing additional charged scalar fields, that being *ad hoc* are not very appealing and furthermore generally worsen the naturalness of the theory. More recently, it was shown that the required ν_h lifetime [18,19] and mass [19] can be naturally obtained in the minimal version of the Supersymmetric Standard Model [6] if one does not forbid R-parity breaking couplings [1] that violate lepton number, thus allowing for the radiative generation of sizeable neutrino masses, magnetic moments and mixings; it was then shown [20] that also in E6 models these neutrino properties can be obtained. However, it was soon realized [21] that the required mass matrix would induce neutrino oscillations which are hardly compatible with the existing experimental limits. Using the Barbieri–Fiorentini bound on neutrino magnetic moments, we will show here that in general the unobservation of neutrino oscillations leave little room for Sciama neutrinos. However, if a cancellation mechanism for the off–diagonal term in the ν mass matrix is provided, R–broken SUSY (and also E6 models) can show the required neutrino properties.

1.3.1 Sciama scenario and neutrino oscillations limits

The existence of interactions which mix the different leptonic flavors can lead to a neutrino mass matrix which is non diagonal in the flavor indices. For simplicity, we consider only the two left handed neutrino flavors ν_1, ν_2 which more significantly contribute to the heaviest mass eigenstate ν_h of mass m_{ν_h} and to its preferred decay product ν_l of mass m_{ν_l}, neglecting the effect of the mixing with the third neutrino flavor, which can be lighter or heavier than ν_l. The decay rate $\Gamma(\nu_h \to \nu_l \gamma)$ for Majorana neutrinos is related to the transition magnetic moment $\mu_{\nu_1\nu_2}$ as follows

$$\Gamma(\nu_h \to \nu_l \gamma) = \frac{\alpha}{8} \frac{m_{\nu_h}^3}{m_e^2} \left[1 - \left(\frac{m_{\nu_l}}{m_{\nu_h}}\right)^2\right]^3 \left|\frac{\mu_{\nu_1\nu_2}}{\mu_B}\right|^2 \tag{1.22}$$

where μ_B is the Bohr magneton.[3] This leads to a lifetime for ν_h (assuming $m_{\nu_l} \ll m_{\nu_h}$)

$$\tau_h = \Gamma^{-1} \simeq \left(\frac{m_{\nu_h}}{28\text{eV}}\right)^{-3} \left|\frac{\mu_{\nu_1\nu_2}}{10^{-14}\mu_B}\right|^{-2} \times 0.9 \cdot 10^{23} s \tag{1.23}$$

So we see that for $m_{\nu_h} \simeq 28$ eV, in order to get $\tau \simeq 1.5 \cdot 10^{23} s$, a magnetic moment $\mu_{\nu_1\nu_2} \sim 10^{-14}\mu_B$ is required. Generally, the contributions to the magnetic moments and to the masses are related. In the Standard Model, if one introduces the right handed neutrinos and allows for tree level Dirac neutrino masses compatible with experiments ($m_{\nu_e} \lesssim 10$ eV) and with cosmology ($\sum m_{\nu_i} \lesssim 100$ eV), the one loop induced magnetic moments result quite small ($\mu \simeq 3 \cdot 10^{-18}(m_\nu/10\text{eV})\mu_B$) [10], so that the radiative neutrino lifetime is too large to produce the required effect by at least seven orders of magnitude.

We have seen in the previous section that in the MSSM with R–parity breaking one can naturally achieve neutrino magnetic moments up to $10^{-13}\mu_B$ even without invoking any particular cancellation mechanism [2]. In fact, it has been shown [18,19] that the usual Minimal SSM (MSSM) with R-parity breaking can lead to the neutrino properties required by the Sciama scenario, however the resulting neutrino mass matrices [19] induce too large neutrino oscillations [21].

[3] Actually, Γ is proportional to $|\mu_{\nu_1\nu_2}|^2 + |d_{\nu_1\nu_2}|^2$, where $d_{\nu_1\nu_2}$ is the transition electric dipole moment [22]. When CP is conserved, if the CP parities of ν_h and ν_l are opposite $d_{\nu_1\nu_2} = 0$. If they are the same, one has $\mu_{\nu_1\nu_2} = 0$ and $\mu_{\nu_1\nu_2}$ should be replaced by $d_{\nu_1\nu_2}$ in all the equations.

In fact, in general the experimental limits on neutrino oscillations severely constrain the Sciama scenario.

Let us analyze the problem in a model independent way. The neutrino mass matrix is

$$\begin{pmatrix} m_{\nu_1\nu_1} & m_{\nu_1\nu_2} \\ m_{\nu_2\nu_1} & m_{\nu_2\nu_2} \end{pmatrix} \tag{1.24}$$

with the Sciama conditions

$$m_{\nu_1\nu_1} \simeq m_{\nu_h} \sim 30\text{eV} \gg m_{\nu_2\nu_2}. \tag{1.25}$$

Taking into account the 90% c.l. limits on the ν mixing angle θ from ν oscillations searches [23], for the mass differences $\Delta m^2 = m^2_{\nu_h} - m^2_{\nu_l} \sim 10^3\text{eV}$ needed by Sciama, we get

$$|m_{\nu_1\nu_2}| \simeq m_{\nu_h} \left|\frac{\sin(2\theta)}{2}\right| < m^{max}_{\nu_1\nu_2} \simeq \begin{cases} 0.8\text{eV}, & \text{for } \nu_1 = \nu_\mu,\, \nu_2 = \nu_e \\ 0.9\text{eV}, & \text{for } \nu_{1,2} = \nu_{\mu,\tau} \\ 5\text{eV}, & \text{for } \nu_1 = \nu_\tau,\, \nu_2 = \nu_e \end{cases} \tag{1.26}$$

On the other hand, the Barbieri–Fiorentini bound (see the Appendix) reads

$$|\delta m_{\nu_1\nu_2}| \gtrsim (g/4\pi^2)\mu_{\nu_1\nu_2}\Lambda^2 \simeq 0.3\text{eV}\frac{\mu_{\nu_1\nu_2}}{10^{-14}\mu_B}\left(\frac{\Lambda}{100\text{GeV}}\right)^2 \tag{1.27}$$

where Λ is a cutoff of the order of the scale where new physics beyond the SM comes into the game, and $g \simeq 0.4$ is the typical electroweak coupling. For $\Lambda \gtrsim 50\text{GeV}$, and for $\mu = 10^{-14}\mu_B$, we get $|\delta m_{\nu_1\nu_2}| \gtrsim 0.075\text{eV}$. We see that the Barbieri–Fiorentini bound leaves enough room for Sciama neutrinos compatibly with the limits from unobserved neutrino oscillations (1.26), especially for $\nu_h = \nu_\tau$ and $\nu_l = \nu_e$. We notice also that this Barbieri–Fiorentini bound can be evaded only if a cancellation mechanism for the contributions to $\delta m_{\nu_1\nu_2}$ is provided, e.g. by a symmetry between ν_1 and ν_2.

1.3.2 Sciama scenario in SUSY with R–parity breaking

Let us consider the case of the SSM with R–parity breaking. We assume that the λs of (1.6) are real, so that they do not violate CP. Fig. 4 shows a generic pair of the one loop diagrams, arising from the purely leptonic couplings in (1.6) that contribute to $m_{\nu_i\nu_j}$, and to $\mu_{\nu_i\nu_j}$ after insertion of a photon vertex on any internal line. Diagrams (a) and (b) must be considered together, and summed, because they are proportional to the same R-breaking coupling constants; for the diagonal matrix elements ($i = j$), if the two flavors running in the loop are the same ($k = k'$), both diagrams coincide, so that just one should be considered. Analogous diagrams exist, originating from the couplings in (1.6) involving the quark fields, with the internal leptons (sleptons) replaced by quarks (squarks). Their contribution is similar to that of fig. 1, so for definiteness we will restrict only to the leptonic one.

FIGURE 4. One loop diagrams contributing to $m_{\nu_i\nu_j}$, and to $\mu_{\nu_i\nu_j}$ (for $i \neq j$) when a photon line is inserted on each internal line.

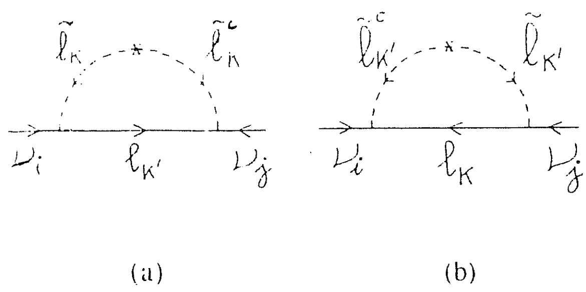

Notice that, while the diagonal neutrino mass terms can be non zero, the corresponding contributions to the diagonal neutrino magnetic moments vanish by Lorentz symmetry. Furthermore, in the diagrams of fig. 1 an helicity flip on the internal fermion line is necessary. As explicitly indicated, this also requires a mixing of the scalar leptons associated with the different chiralities, described by the scalar Lagrangian term $\Delta_{ij}\tilde{l}_i\tilde{l}^c_j$. To be more predictive, we will consider the MSSM[4] in which every contribution to the mixing square mass matrix Δ is proportional to the fermionic lepton mass matrix diag(m_e, m_μ, m_τ) as in eq. (1.7), and the sleptons are degenerate at a mass m_0.

The generic single diagram of fig. 1 (a) contributes to $m_{\nu_i\nu_j}$ and $\mu_{\nu_i\nu_j}$ (after insertion of the photon line) respectively as

$$\delta m_{\nu_i\nu_j} \simeq \frac{\lambda_a\lambda_b}{16\pi^2} m_{k'} \frac{\Delta_{kk}}{m_0^2} \tag{1.28}$$

$$|\delta\mu_{\nu_i\nu_j}| = \mu_B \frac{\lambda_a\lambda_b}{2\pi^2}\frac{m_e m_{k'}}{m_0^2}\left(\ln\left(\frac{m_0}{m_{k'}}\right) - 1\right)\frac{\Delta_{kk}}{m_0^2} \qquad (\text{for } i \neq j) \tag{1.29}$$

where $m_{k'}$ is the mass of the internal charged fermionic lepton, λ_a and λ_b are the appropriate couplings, and Δ_{kk} is the relevant mixing term of the scalar line. The contribution of graph 1 (b) has the same form of this one, if the substitution $k \leftrightarrow k'$ is done.

For simplicity, for a fixed pair (i, j) we will consider only the contributions $\delta m_{\nu_i\nu_j}$ due to the graphs of the kind given in fig. 1 which are proportional to the largest value of the product $\lambda_a\lambda_b m_{k'}\Delta_{kk}$. Then for the entry $m_{\nu_1\nu_2}$ of the mass

[4] From ref. [18] we know that in a more general SSM there are not better possibilities for Sciama neutrinos.

matrix corresponding to the two neutrino flavors ν_1, ν_2 we can write

$$m_{\nu_1\nu_2} \simeq 4.9\text{eV} \left(\frac{m_0}{100\text{GeV}}\right)^2 \left|\frac{\mu_{\nu_1\nu_2}}{10^{-14}\mu_B}\right| \left[\frac{10}{\ln\left(m_0^2/(mm')_{12}\right) - 2}\right] \tag{1.30}$$

where $(mm')_{12}$ is the product $m_k m_{k'}$ for the indices k, k' which correspond to the main contribution to the entry $m_{\nu_1\nu_2}$. Then by eq. (1.28) the full ν_1, ν_2 mass matrix is determined (given the values of the λ's and m_0),

$$\begin{aligned} m_{\nu_1\nu_1} &\simeq \left(\frac{1}{2}\right) \frac{(\lambda\lambda mm')_{(11)}}{(\lambda\lambda mm')_{(12)}} m_{\nu_1\nu_2} \\ m_{\nu_2\nu_2} &\simeq \left(\frac{1}{2}\right) \frac{(\lambda\lambda mm')_{(22)}}{(\lambda\lambda mm')_{(12)}} m_{\nu_1\nu_2} \end{aligned} \tag{1.31}$$

where the factor $\left(\frac{1}{2}\right)$ corresponds to the case in which both particles in the loop for the diagonal matrix element have the same flavor. It is clear that, provided that the coupling constants can be large enough to give an eigenvalue $m_{\nu_h} \simeq 28$ eV, it is easy to find ratios of the masses and/or coupling constants which give $m_{\nu_l} \ll m_{\nu_h}$ and, by construction, guarantee the wanted lifetime for ν_h. However, from (1.30) the limit (1.26) can be satisfied only for $\nu_h = \nu_\tau$, $\nu_l = \nu_e$, and for $m_{\tilde{l}} < 100$GeV. Furthermore, since now the heavy entry $m_{\nu_\tau\nu_\tau}$ of the mass matrix can be obtained only by the exchange of a pair $\mu\tilde{\mu}$ due to the asymmetric form of the couplings λ, in order to get $m_{\nu_h} \simeq 28$ eV a value of λ_{232} which slightly exceeds the bound $< .09(m_0/100\text{GeV})$ of ref. [8] is necessary.

It can be shown that the situation does not improve considering the quark–squark loops, proportional to products $\lambda'\lambda'$. In fact, in this case the limit (1.26) cannot be satisfied neither for $\nu_h = \nu_\tau$, $\nu_l = \nu_e$ (an additional factor 3 of colour is present, and the region $m_{\tilde{q}} < 100$GeV is experimentally excluded). Only if a cancellation mechanism on $m_{\nu_1\nu_2}$ is provided one can have Sciama neutrinos in these models. Clearly, the parameter space remains limited, so that the naturalness of the model is lost.

1.4 Conclusions

In theories which extend the SM, L and L_e, L_μ, L_τ conservations are no longer consequences of minimal particle content and gauge structure. For instance, in SUSY theories with broken R–parity new L and L_i violating vertices exist, with two ordinary fermion legs and one scalar leg corresponding to a superpartner.

We have shown that a neutrino magnetic moment as large as $\mu_{\nu_e \nu_\mu} \sim 10^{-13}\mu_B$ can be obtained naturally in the MSSM with such L–violating vertices; an order of magnitude can be gained in non–minimal SSM with an additional family symmetry broken by the Yukawa mass term of the muon.

We have then considered the Sciama scenario in which an heavy neutrino ν_h of mass $m_{\nu_h} \simeq 28$eV decays radiatively in a much lighter neutrino ν_l with lifetime $\tau \sim 10^{23}s$. The experimental constraints on neutrino oscillations and the Barbieri–Fiorentini theoretical limit on neutrino magnetic moments leave a little room to realize the scenario; in the particular case of R–broken SUSY these two conditions cannot be satisfied simultaneously, unless an additional symmetry is invoked to partially cancel the off–diagonal neutrino mass entry.

The models considered in this chapter have been proved to be a fertile field especially for the interesting neutrino properties they lead to. Besides the exemples examined here, it is worth mentioning the recent observation by Roulet [24] that in these models the flavour changing interactions can produce matter enhanced neutrino oscillations, explaining the solar neutrino deficit, even in the absence of vacuum mixing. This proposal has then been further examined in references [25]; very recently, it was shown that this kind of MSW effect without vacuum oscillations can be obtained also in E6 models [26].

Recently it has been shown that the R–parity breaking interactions would wash out the cosmological matter-antimatter asymmetry [27]. The resulting constraint $|\lambda| \lesssim 10^{-8}$ on the coupling constants λ and λ' would deprive these models of phenomenological interest. However, it has been argued [28] that these limits could be escaped either by regenerating the erased cosmological B asymmetry after the electroweak phase transition, or by the spontaneous breaking of R_p at a temperature where non perturbative effects are no longer capable of producing B and L violation at a too high rate [29].

Appendix A

Relation between neutrino mass and magnetic moment

The magnetic moment operator corresponds to the effective interaction

$$\mu\nu_1\sigma_{\alpha\beta}\nu_2 F_{\alpha\beta}, \qquad (A.1)$$

where $F_{\alpha\beta}$ is the electromagnetic field strenght. This operator destroys the two left–handed fields ν_1 and ν_2; equivalently it destroys e.g. ν_1 and creates $(\nu_2^c)_R$, so that it corresponds to a chirality flip, just like a mass term. ν_1 and ν_2 can belong to $SU(2)_L$ doublets, as it would happen if no right–handed is introduced, like in the models we consider in chapter 1; however, our argument works unchanged if one of them is a singlet.

There is a theoretical, Ward–like, relation between the neutrino magnetic moment and the mass [3]. A sizeable value $\mu = \mu_{\nu_1\nu_2}$ of an entry of the neutrino magnetic moment matrix would induce a contribution $\delta m = \delta m_{\nu_1\nu_2}$ to the neutrino mass entry which has the same fermionic external lines.

Such magnetic moment should originate from some new physics, occurring at a scale $\Lambda \gtrsim 50$GeV. At lower energies, $SU(2)_L \times U(1)_Y$ invariance implies that if the magnetic interaction (A.1) exist, there is also the Z interaction

$$\mu\nu_1\sigma_{\alpha\beta}\nu_2 Z_{\alpha\beta}, \qquad (A.2)$$

where $Z_{\alpha\beta}$ is the Z–boson field strenght. Then the graph of figure 1 will contribute to the mass m, and its contribution will be of the order

$$\delta m \simeq \frac{g}{4\pi^2}\mu\Lambda^2 \qquad (A.3)$$

where g is the coupling to the Z boson. Clearly, this is also an estimate of the minimum value of the mass entry m, if no cancellation (i.e., fine tuning) with other contributions occur.

FIGURE 1. A contribution to $m_{\nu_1\nu_1}$ corresponding to $\mu_{\nu_1\nu_2}$.

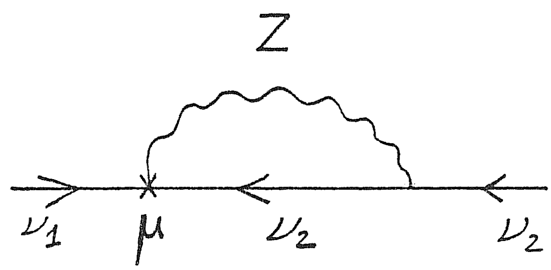

The neutrino mass entries are limited by the bounds on the ν masses and oscillation experiments, so that eq. (A.3) gives a constrain on the magnetic moment, taking into account that $\Lambda \gtrsim 50\text{GeV}$. For instance, if $\nu_1 = \nu_e$ there is typically a limit $m \lesssim 10\text{eV}$, so that the bound $\mu \lesssim 10^{-13}\mu_B$ is obtained.

In most of the models which have been considered to get large magnetic moments, both the mass and magnetic moment are generated at one loop. A graph for the magnetic moment contributes also to the mass when the photon leg is removed. Then by dimensional analysis the magnetic moment and mass can be estimated to be

$$\delta\mu \sim \frac{e\mathcal{G}}{M}, \qquad \delta m \sim \mathcal{G}M \tag{A.4}$$

where $\mathcal{G}$ is some constant depending on the couplings entering the graph. We get then

$$\delta m \sim \frac{M^2}{e}\delta\mu \tag{A.5}$$

which is to be compared to (A.3).

Both eqs. (A.3) and (A.5) imply that the neutrino magnetic moment must be much lower than the value required by the Voloshin–Vysotskii–Okun [30] explanation of the observed solar neutrino flux time variation. However, larger magnetic moments can be obtained if a symmetry ensuring cancellation of different mass contributions is provided [11]. If such 'Voloshin' symmetry exists, the limits discussed in this appendix are no more compelling.

Chapter 2

Precision Tests of the Standard Model

Precision measurements have tested the SM of electroweak interactions in the last decade. Experimental uncertainties $\lesssim 1\%$ have been reached for several observables, allowing to probe even the quantum structure of the theory. The electroweak radiative corrections at 1–loop, improved by leading higher order effects, must be included in the expressions to be compared with experiments, to get the needed theoretical uncertainties of the order $0.1 - 1\%$.

The great number of independent measures of the particles masses and effective couplings, performed at several energy scales and from many different processes, has been proved to be very powerful to test almost all the sectors of the SM lagrangian, and to severely constrain (or exclude) possible 'new', i.e. non–standard, physics. However, there are still some important missing points. The Higgs sector of the theory is poorly tested experimentally, and the top–quark has not yet been produced. By now, only lower limits on the Higgs and top–quark masses have been obtained. However, if these particles exist, they will run into loops, and their contribution to the radiative corrections for the gauge bosons propagators and for the effective couplings will be eventually bigger than the experimental accuracies. In particular an heavy top–quark will significantly contribute, then precision measurements allow also to determine preferred ranges for its mass. On the other hand, the lack of knowledge of the top (and to a smaller extent of the Higgs) masses is just one of the major sources of uncertainty in the theoretical predictions within the SM.[5]

In this chapter, we will discuss the SM expectations and the experimental values for a large set of precision measurements, following ref. [31]. Experimental errors have been evaluated by adding statistical and systematic uncertainties in quadrature and correlations have been taken into account in all the relevant cases. Our aim is mainly to provide the basis for the fit to a class of models which extend the SM, which we will perform in chapter 4. However, we will also present here, as a first application, the result of the fit for the top mass in the framework of the SM.

We will briefly define the renormalisation scheme used for the computation of the SM radiative corrections in section 1; the Charged Current (CC) and the Neutral Current (NC) experiments will be discussed in sections 2 and 3 respectively; in section 4 we will present the results of the very recent NC experiments performed at the Z–peak; finally in section 5 we will give the result of the fit for the top mass in the SM using all this set of data.

2.1 Renormalisation of the SM

Several renormalisation schemes have been used to compute measurable quantities

[5] Another sector of the SM which is still waiting for experimental probes is the one of the non abelian couplings among gauge bosons.

in the SM. Here a renormalisation scheme is defined by a choice of an independent set of parameters which define the theory.[6] The scheme dependence of the electroweak radiative correction, computed at a given order in perturbation theory, is discussed for instance in ref. [32]. The precision of $\sim 0.1\%$ can be reached in every scheme at one loop adding the appropriately resummed leading higher order effects.

To get accurate physical predictions, it is convenient to use a set of parameters which can be measured directly, preferably the most precisely determined ones. Hence we will choose the input parameters $\{\alpha, G_\mu, M_Z, m_f, m_H, V_{ij}\}$, where m_f is the set of fermion masses and V is the Cabibbo–Kobayashi–Maskawa (CKM) quark mixing matrix. The fine structure constant $\alpha = e^2/4\pi = 1/137.0359895(61)$ is the eletromagnetic strenght at low energy, measured in Coulomb scattering for vanishingly small momentum transfer (Thomson limit). The Z–mass is also known with high precision, $M_Z = 91.175 \pm 0.021$ GeV [33]. $G_\mu = 1.16637(2) \times 10^{-5}\mathrm{GeV}^{-2}$ [23] is the Fermi coupling constant at the energy scale m_μ, $G_\mu = G_F(m_\mu)$, extracted from the life–time $\tau_\mu = 2.197035(40) \times 10^{-6}s$ of the μ-lepton,

$$\tau_\mu^{-1} \equiv \frac{G_\mu^2 m_\mu^5}{192\pi^3} f\left(\frac{m_e^2}{m_\mu^2}\right)\left(1+\frac{3m_\mu^2}{5m_W^2}\right)\left[1+\frac{\alpha(m_\mu)}{2\pi}(\frac{25}{4}-\pi^2)\right], \qquad (2.1)$$

where $\alpha(m_\mu)$ is the electromagnetic strenght at the energy m_μ,

$$\alpha(m_\mu) = \alpha(1 + \frac{2\alpha}{3\pi}\log\frac{m_\mu}{m_e}), \qquad (2.2)$$

and

$$f(x) = 1 - 8x + 8x^3 - x^4 - 12x^2\log x. \qquad (2.3)$$

[6] This definition is different from the other usual, more technical one, as discussed e.g. in ref. [32].

The scheme outlined above differs from the natural *on–shell* scheme, analogous to the one used in QED, which uses the less accurate measurement of M_W instead of G_μ. However, we can use the value of M_W predicted in the scheme with G_μ and then compute radiative corrections in the *on–shell* scheme [32]. The theoretical expression for the W mass reads [34]

$$M_W^2 = \frac{\rho M_Z^2}{2}\left[1+\sqrt{1-\frac{4\mathcal{A}}{\rho M_Z^2}\left(\frac{1}{1-\Delta\alpha}+\Delta r^{rem}\right)}\right], \tag{2.4}$$

where $\mathcal{A} = \pi\alpha/\sqrt{2}G_\mu$. The $1/(1-\Delta\alpha)$ term renormalizes the QED low energy coupling to the M_Z scale and resums to all orders the large logs contained in the photon vacuum polarization function. The leading top effects, quadratic in m_t, are included in the parameter $\rho \simeq \rho_{top} = 1 + 3G_\mu m_t^2/8\sqrt{2}\pi^2$ [35], which measures the ratio of the NC low–energy strenght to the CC strenght G_μ. We have taken $\rho = 1$ at the tree level, that corresponds to the absence of non–doublet Higgs VEV's and of extra $U(1)$ gauge bosons with non–zero mixing with the standard Z. The non-leading top and Higgs effects and other small corrections are included in the Δr^{rem} term. We refer to [36] for a detailed discussion of all these corrections.

SM 1–loop radiative corrections can be divided into two subclasses:

i) 'QED corrections' involving the emission of real photons or the exchange of virtual photons in loops, but not including vacuum polarisation diagrams. These graphs yeld large, but finite and gauge–invariant contributions to observable processes. However they depend on energies, experimental cuts, etc., and must be calculated individually for each experiment.

ii) 'Electroweak corrections', collecting all the other 1–loop diagrams: $\gamma\gamma, \gamma Z, ZZ$ and WW vacuum polarition diagrams, vertex corrections, box graphs, etc. They are independent of experimental cuts, but are sensitive to new physics beyond the SM.

In the rest of this chapter, we will be mainly concerned with the electroweak corrections, but it is understood that the (usually larger) QED corrections have been taken into account for extracting the values of the various observables from experiments (fortunately, this has often been done by the data analyses of the experimental collaborations).

2.2 Charged Currents

The weak CC interaction lagrangian is

$$\begin{aligned} \mathcal{L}^{CC}_{int} =& (\frac{G_\mu}{\sqrt{2}} M^2_W)^{1/2} (J^+_\mu W^{-\mu} + h.c.), \\ J^+_\mu =& \sum_{i=1}^{3} \bar{\nu}_{iL} \gamma_\mu e_{iL} + \sum_{i,j=1}^{3} \bar{u}_{iL} V_{ij} \gamma_\mu d_{jL}. \end{aligned} \tag{2.5}$$

A first experimental constraint is given by the measurement of the W–mass itself, whose theoretical SM expression has been given in eq. (2.4). Experimentally the value of the W mass, as measured by CDF, is $M_W = 79.91 \pm 0.39$ GeV [37]. The UA2 collaboration has measured the ratio of the W and Z masses, for which many systematic errors cancel, obtaining $M_W/M_Z = 0.8831 \pm 0.0055$ [37]. Using the LEP value for M_Z and averaging the two results yields

$$M_W = 80.13 \pm 0.31 \text{GeV}. \tag{2.6}$$

We will then consider three different kinds of CC experimental constraints: i) lepton universality; ii) CKM unitarity; iii) limits on Right Handed Currents (RHC).

i) Lepton universality

The ratios g_μ/g_e and g_τ/g_e of the leptonic couplings to the W boson, which in the SM are predicted to be unity (universality), can be determined experimentally by comparing two different leptonic decay processes.

1) In $p\bar{p}$ collisions, $(g_i/g_e)^2$ are extracted from the ratios of the partial cross sections

$$\frac{\sigma(p\bar{p}\to W)B(W\to l_i\nu_i)}{\sigma(p\bar{p}\to W)B(W\to e\nu_e)}=\left(\frac{g_i}{g_e}\right)^2, \qquad i=\mu,\tau. \tag{2.7}$$

The weighted average of the UA1 and UA2 [38] measurements is given in table I.

2) In the leptonic decays $(l_i\to l_j\nu\bar{\nu})$, we get

$$\begin{aligned}\frac{\Gamma(\tau\to\mu\nu\bar{\nu})}{\Gamma(\tau\to e\nu\bar{\nu})}&=\left(\frac{g_\mu}{g_e}\right)^2\frac{f(\frac{m_\mu^2}{m_\tau^2})(1+\frac{3m_\mu^2}{5m_W^2})}{f(\frac{m_e^2}{m_\tau^2})(1+\frac{3m_e^2}{5m_W^2})},\\ \frac{\Gamma(\tau\to\mu\nu\bar{\nu})}{\Gamma(\mu\to e\nu\bar{\nu})}&=\left(\frac{g_\tau}{g_e}\right)^2\frac{m_\tau^5 f(\frac{m_\mu^2}{m_\tau^2})(1+\frac{3m_\mu^2}{5m_W^2})[1+\frac{\alpha(m_\tau)}{2\pi}(\frac{25}{4}-\pi^2)]}{m_\mu^5 f(\frac{m_e^2}{m_\mu^2})(1+\frac{3m_e^2}{5m_W^2})[1+\frac{\alpha(m_\mu)}{2\pi}(\frac{25}{4}-\pi^2)]},\end{aligned} \tag{2.8}$$

with $\alpha(m)$ and $f(x)$ given by (2.2) and (2.3). The values of $g_{\tau,\mu}/g_e$ can then be evaluated using the experimental determinations of the τ branching fractions into e and μ and the measured τ–lifetime [23]. Combining the averages of [23] with two very recent measurement of the L3 and OPAL collaborations [39] we obtain [31] $Br(\tau\to\mu\nu_\mu\nu_\tau)=0.1752\pm0.0032$ and $Br(\tau\to e\nu_e\nu_\tau)=0.1775\pm0.0032$ from which the values in table I are derived.

We notice that the value of g_τ/g_e is almost 2σ off the SM value. This is due to the fact that the measured τ lifetime is about 2σ bigger than the theoretical computation. This could be a signal of new physics [40], or it could be due to problems with the experimental normalisations [41,42].

3) Finally, also the π and K leptonic decays constrain universality of the μ and e couplings, through the ratios

$$\frac{\Gamma(\pi \to \mu\nu)}{\Gamma(\pi \to e\nu)} = \left(\frac{g_\mu}{g_e}\right)^2 \left(\frac{m_\mu}{m_e}\right)^2 \left(\frac{m_\pi^2 - m_\mu^2}{m_\pi^2 - m_e^2}\right)^2 \left(1 - \frac{3\alpha}{\pi}\log\frac{m_e}{m_\mu}\right), \tag{2.9}$$

(and similarly for $\Gamma(K \to \mu\nu)/\Gamma(K \to e\nu)$) where several theoretical uncertainties cancel. The experimental values computed from the averages reported in [23], are also shown in table I.

TABLE I. Charged Current experimental constraints on lepton universality (g_i/g_e), unitarity of the quark mixing matrix V_{ij}, and induced hadronic RHC (κ_{ij}).

Quantity	Experimental value	Correlation	Processes
$(g_\mu/g_e)^2$	1.00 ± 0.20		$W \to l\nu$
$(g_\tau/g_e)^2$	1.00 ± 0.12		
$(g_\mu/g_e)^2$	1.016 ± 0.026	0.40	$\tau \to l\nu\bar{\nu}$
$(g_\tau/g_e)^2$	0.952 ± 0.031		and $\mu \to e\nu\bar{\nu}$
$(g_\mu/g_e)^2$	1.014 ± 0.011		$\pi \to l\nu$
"	1.013 ± 0.046		$K \to l\nu$
$\sum_{i=1}^3 \lvert V_{ui}\rvert^2$	0.9981 ± 0.0021		hadrons decays
$\sum_{i=1}^3 \lvert V_{ci}\rvert^2$	1.08 ± 0.37		ν-d scatt. and D_{e3}
$\mathrm{Re}(\kappa_{ud})$	0 ± 0.0037		$K \to 3\pi, 2\pi$
$\mathrm{Re}(\kappa_{us})$	0 ± 0.0037		

ii) CKM unitarity

The unitarity sums $\sum_{i=1}^{3}|V_{ui}|^2$ and $\sum_{i=1}^{3}|V_{ci}|^2$, are constrained in the SM to be unity. Their experimental determinations provide an important test of the SM, constraining also the possible new physics which could make the sums different from 1.

The best determination of $|V_{ud}|$ comes from superallowed nuclear beta–decays, which are induced by the vector part of the weak current, and is $|V_{ud}| = 0.9744 \pm 0.0010$. The error has mainly a theoretical origin, since non–universal radiative corrections (i.e., depending on the nucleus considered), as well as universal corrections, are important. Recent analyses [43] report a reduced error on $|V_{ud}|$, but due to the persistent theoretical confusion [44,42], we have choosen the more conservative value of [23]. The value $|V_{us}| = 0.2205 \pm 0.0018$ is obtained by averaging the determination from K_{e3} decays with the value from the hyperon decay [23].

$|V_{cd}|$ can be deduced from the production rate of charm in neutrino–nucleon scattering ($\nu d \to \mu^- c$). In the quark–parton model, the cross sections for the di–muon charm production in neutrino and antineutrino scattering off the average, 'isoscalar' nucleon of mass M are

$$\begin{aligned}
\sigma^{\nu}_{\mu^-\mu^+} &= \frac{G_\mu^2 M E_\nu}{\pi}\left[|V_{cd}|^2(U+D) + |V_{cs}|^2 2S\right] B(c\to\mu),\\
\sigma^{\bar\nu}_{\mu^+\mu^-} &= \frac{G_\mu^2 M E_{\bar\nu}}{\pi}\left[|V_{cd}|^2(\bar U+\bar D) + |V_{cs}|^2 2\bar S\right] B(c\to\mu),
\end{aligned}$$

where U, D, S denote the quark content of the isoscalar target [45], consisting of valence parts and 'sea' parts $\bar U, \bar D, \bar S$ (such that $U = D$, $\bar U = \bar D$, $U - \bar U + D - \bar D = 3$, and $S = \bar{S}$). On the other hand, the total cross sections for muon production are

$$\sigma^{\nu}_{\mu^-} = \frac{G_\mu^2 M E_\nu}{\pi}\left[U + D + S + \frac{\bar{U}+\bar{D}}{3}\right],$$
$$\sigma^{\bar{\nu}}_{\mu^+} = \frac{G_\mu^2 M E_{\bar{\nu}}}{\pi}\left[\frac{U+D}{3} + \bar{U} + \bar{D} + \bar{S}\right].$$

Hence,

$$B(c \to \mu)|V_{cd}|^2 = \frac{\sigma^{\nu}_{\mu^-\mu^+} - \sigma^{\bar{\nu}}_{\mu^+\mu^-}}{\sigma^{\nu}_{\mu^-} - \sigma^{\bar{\nu}}_{\mu^+}}\frac{2}{3}.$$

The resulting value for V_{cd} is $|V_{cd}| = 0.204 \pm 0.017$ [23].

$|V_{cs}|$ also is obtained by neutrino production of charm; however there is another determination from D_{e3} decays, and the average is $|V_{cs}| = 1.02 \pm 0.18$, taking the conservative value of ref. [23]. The values of V_{ub} and V_{cb} are found to be so small [23], that they do not contribute significantly to the unitarity sums, so that we obtain the results of table I for the CKM untarity constraints.

iii) Right handed currents

Right Handed Charged Currents (RHC) do not exist in the pure SM. Let us assume that, besides the usual CKM matrix, there exist a matrix $V_{Rij} = k_{ij} V_{ij}$ which describes the right–handed current for the quarks,

$$J_\mu^+ = \sum_{i=1}^{3} \bar{\nu}_{iL}\gamma_\mu e_{iL} + \sum_{i,j=1}^{3} \bar{u}_{iL} V_{ij}(P_L + k_{ij}P_R)\gamma_\mu d_{jL}.$$

Very stringent limits on the k_{ud} and k_{us} RHC's were set [46] from the observation that the $K \to 3\pi$ amplitude and slope parameters are predicted, within an accuracy of $\sim 10\%$, by PCAC and by the measured $K \to 2\pi$ matrix elements. The resulting limits

$$|k_{ud}|, |k_{us}| < \frac{8 \times 10^{-4}}{|V_{ud}||V_{us}|} \simeq 0.0037 \qquad (2.10)$$

are treated as 1σ experimental constraints [47] on $|\kappa_{ud}|$ and $|\kappa_{us}|$ in table I.

Limits on the k_{cd} and k_{cs} RHC's were set by the CDHS collaboration [45] from the analysis of the y distribution in the di-muon charm production in neutrino scattering off nuclei. y is the fraction of the initial neutrino energy which is absorbed by the hadrons, and possible right–handed currents are caracterized by the $(1-y)^2$ behaviour,

$$\frac{d\sigma^{\nu}_{\mu^-\mu^+}}{dy} = \frac{G_\mu^2 M E_\nu}{\pi}\{\left[|V_{cd}|^2(U+D) + |V_{cs}|^2 2S\right] \\ + \left[|V_{Rcd}|^2(U+D) + |V_{Rcs}|^2 2S\right](1-y)^2\}B(c\to\mu).$$

The experimental limit on the $(1-y)^2$ term gave [45] the following 95% confidence level bound

$$\frac{|k_{cd}|^2 + |k_{cs}|^2 \left|\frac{V_{cs}}{V_{cd}}\right|^2 \frac{2S}{U+D}}{1+\left|\frac{V_{cs}}{V_{cd}}\right|^2 \frac{2S}{U+D}} < 0.07. \qquad (2.11)$$

Using the experimental estimate [45] for $\left|\frac{V_{cs}}{V_{cd}}\right|^2 \frac{2S}{U+D}$ we can derive from this bound an experimental constraint on the parameters κ_{cd} and κ_{cs}.

The leptonic RHC's are limited by the measurements of the μ and τ Michel parameters, as well as by the electron polarization in β decays (see e.g. the analyses in [48,23,49]).

2.3 Neutral currents

The Neutral Current interaction between the fermion current and the Z is given by the Lagrangian

$$\mathcal{L}_Z = -\left(\sqrt{2}G_\mu M_Z^2\right)^{1/2} \sum_f \bar{\Psi}_f\gamma_\mu(v_f - a_f\gamma_5)\Psi_f\ Z^\mu, \qquad (2.12)$$

with

$$\begin{aligned} v_f &= t_3^f - 2Q^f s_W^2 \\ a_f &= t_3^f \end{aligned} \tag{2.13}$$

where $c_W^2 \equiv 1 - s_W^2 \equiv m_W^2/m_Z^2$, and we will retain this definition of s_W to all orders in perturbation theory. The main effects of electro–weak radiative corrections, in the precision NC experiments we will consider, can be accounted for

1) by replacing the vector couplings v_f with the effective couplings

$$v_f^i = t_3^f - 2Q^f k_i s_W^2 \tag{2.14}$$

where the correction κ_i depends on the particular i^{th} experiment considered, and has an universal contribution quadratic in the top mass, $\kappa_{top} = 1 + 3G_\mu \frac{c_W^2}{s_W^2} m_t^2/8\sqrt{2}\pi^2$;

2) by multiplying the NC amplitudes by a ρ_i parameter, depending again on the i^{th} process considered, and which has an universal contribution equal to the ρ_{top} introduced above (see comment after eq. (2.4));

3) there are then other residual corrections, like the λ_{qL} and λ_{qR} we will introduce below.

Neutral Current experimental results are conveniently given as fits to the couplings appearing in the effective Lagrangians that describe the corresponding four–fermion processes [23]. The form of these effective Lagrangians relies only on the assumption of spin–one gauge boson exchange and of massless left–handed neutrinos, and thus the experimental values of the phenomenological parameters are essentially model independent.

We will treat separately the $\nu - q$, $\nu - e$ and the parity–violating $e - q$ sectors.

i) Neutrino – quark sector

The effective Lagrangian for the neutral current interaction of the light neutrinos with quarks is

$$-\mathcal{L}^{\nu q} = \frac{G_\mu}{\sqrt{2}}\,\bar{\nu}\gamma_\mu(1-\gamma_5)\nu\ \left[\epsilon_L(q)\bar{q}\gamma_\mu(1-\gamma_5)q + \epsilon_R(q)\bar{q}\gamma_\mu(1+\gamma_5)q\right]. \qquad (2.15)$$

The SM expressions for the effective parameters $\epsilon_a(q)$ can be given in terms of the effective vector couplings $v_q^{\nu N} = t_3^q - 2Q^q\kappa_{\nu N}s_W^2$, with $\kappa_{\nu N} \simeq \kappa_{top} - 0.0027$ (for $m_H = 100$GeV). Introducing also the $\rho_{\nu N}$–correction ($\rho_{\nu N} \simeq \rho$), they read

$$\begin{aligned}\epsilon_L(q) &= \rho_{\nu N}\left[v_q^{\nu N} + a_q^{\nu N} + \lambda_{qL}\right]\\ \epsilon_R(q) &= \rho_{\nu N}\left[v_q^{\nu N} - a_q^{\nu N} + \lambda_{qR}\right]\end{aligned} \qquad (2.16)$$

($q = u, d$) with the further radiative–corrections parameters $\lambda_{uL} \simeq -0.0031$, $\lambda_{dL} \simeq -0.0026$, $\lambda_{uR} = \frac{1}{2}\lambda_{dR} \simeq 3.5 \times 10^{-5}$.

The values of the quark couplings $\epsilon_{L,R}(q)$ are extracted from deep–inelastic scattering experiments off isoscalar and proton targets, normalized to the charged current cross sections, i.e. from the ratios

$$\begin{aligned}R_\nu &= \frac{\sigma(\nu_\mu N \to \nu X)}{\sigma(\nu_\mu N \to \mu^- X)}\\ R_{\bar\nu} &= \frac{\sigma(\bar\nu_\mu N \to \bar\nu X)}{\sigma(\bar\nu_\mu N \to \mu^+ X)}\\ r_\nu &= \frac{\sigma(\nu_\mu p \to \nu X) - \sigma(\nu_\mu n \to \nu X)}{\sigma(\nu_\mu p \to \mu^+ X) - \sigma(\nu_\mu n \to \mu^- X)}\\ r_{\bar\nu} &= \frac{\sigma(\bar\nu_\mu p \to \bar\nu X) - \sigma(\bar\nu_\mu n \to \bar\nu X)}{\sigma(\bar\nu_\mu p \to \mu^+ X) - \sigma(\bar\nu_\mu n \to \mu^- X)}\end{aligned} \qquad (2.17)$$

The experimental values [23] are given in table II in terms of

$$g_a^2 \equiv \epsilon_a(u)^2 + \epsilon_a(d)^2 \quad , \quad \theta_a \equiv \tan^{-1}\left[\frac{\epsilon_a(u)}{\epsilon_a(d)}\right] \qquad a = L, R \qquad (2.18)$$

that have negligible correlations.

ii) Neutrino – electron sector

The effective Lagrangian for the $\nu - e$ sector is

$$-\mathcal{L}^{\nu e} = \frac{G_\mu}{\sqrt{2}}\, \bar{\nu}\gamma_\mu(1-\gamma_5)\nu\, \bar{e}\gamma_\mu(g_V^e - g_A^e\gamma_5)e. \tag{2.19}$$

The SM expressions for the effective parameters g_V^e and g_A^e can be given in terms of the effective vector couplings $v_e^{\nu e} = t_3^e - 2Q^e\kappa_{\nu e}s_W^2$, with $\kappa_{\nu e} \simeq \kappa_{top} - 0.0031$ (for $m_H = 100\text{GeV}$). Introducing also the $\rho_{\nu e}$–correction ($\rho_{\nu e} \simeq \rho_{top} + 0.0047$), they read

$$\begin{aligned} g_V^e &= \rho_{\nu e} v_e^{\nu e} \\ g_A^e &= \rho_{\nu e} a_e^{\nu e}. \end{aligned}$$

The electron vector and axial–vector couplings are extracted from $\nu_\mu e \to \nu_\mu e$ and $\nu_\mu e \to \nu_\mu e$ elastic scattering experiments that, as in the previous case, are normalized with the ν_μ–hadron charged–current cross sections. The cross sections are

$$\begin{aligned} \frac{d\sigma(\nu_\mu e \to \nu_\mu e)}{dy} &= \frac{G_\mu^2 m_e E_\nu}{2\pi}[(g_V^e + g_A^e)^2 + \\ &\qquad (g_V^e - g_A^e)^2(1-y)^2 - (g_V^{e2} - g_A^{e2})\frac{y m_e}{E_\nu}], \\ \frac{d\sigma(\bar{\nu}_\mu e \to \bar{\nu}_\mu e)}{dy} &= \frac{G_\mu^2 m_e E_{\bar{\nu}}}{2\pi}[(g_V^e - g_A^e)^2 + \\ &\qquad (g_V^e + g_A^e)^2(1-y)^2 - (g_V^{e2} - g_A^{e2})\frac{y m_e}{E_\nu}], \end{aligned}$$

where $y = E_e/E_{\nu(\bar{\nu})}$ is the ratio of the recoil electron to the incident ν or $\bar{\nu}$ energy.

In table II we list the values of $g_{V,A}^e$ that we have used [31]. The recent CHARM II [50] results, as well as the CHARM I [51] and BNL [52] data on both

TABLE II. Neutral Current experimental constraints.

Deep-inelastic ν-q		
g_L^2	0.2977 ± 0.0042	
g_R^2	0.0317 ± 0.0034	
θ_L	2.50 ± 0.03	
θ_R	$4.59 {}^{+\,0.44}_{-\,0.27}$	
ν-e scattering		experiment
g_V^e/g_A^e	0.047 ± 0.046	CHARM II
g_V^e	-0.06 ± 0.07	CHARM I
g_A^e	-0.57 ± 0.07	"
g_V^e	-0.10 ± 0.05	BNL
g_A^e	-0.50 ± 0.04	"
e-q parity violation		correlation
C_{1u}	-0.249 ± 0.066	-0.99 -0.95
C_{1d}	0.391 ± 0.059	0.95
$C_{2u} - \frac{1}{2}C_{2d}$	0.21 ± 0.37	

ν_μ and $\bar{\nu}_\mu$ scattering off electrons have all been included. In particular, CHARM II has measured g_V^e/g_A^e from the ratio between ν and $\bar{\nu}$ NC cross sections (no normalisation with the CC rate), leading to a clean measurement of v_e/a_e.

iii) Electron – quark sector

The measurements of parity violation effects in atoms and the polarized $e-D$ scattering experiments are sensitive to weak–electromagnetic interference effects and allow the determination of the $e-q$ parity violating couplings $C_{1,2}$. These parameters appear in the effective Lagrangian

$$-\mathcal{L}^{eq} = -\frac{G_\mu}{\sqrt{2}} \sum_i (C_{1i}\bar{e}\gamma_\mu\gamma^5 e\ \bar{q}^i\gamma^\mu q^i + C_{2i}\bar{e}\gamma_\mu e\ \bar{q}^i\gamma^\mu\gamma^5 q^i), \qquad (2.20)$$

where $i = u, d$. The SM theoretical couplings are $v_q^{eq} = t_3^q - 2Q^f\kappa'_{eq}s_W^2$ and $v_e^{eq} = t_3^e - 2Q^f\kappa_{eq}s_W^2$ with $\kappa'_{\nu e} \simeq \kappa_{top} + 0.0018$ and $\kappa_{\nu e} \simeq \kappa_{top} + 0.037$ (for $m_H = 100\text{GeV}$). The resulting SM expressions for the parameters of the effective lagrangian are then

$$\begin{aligned} C_{1q} &= 2\rho'_{eq}a_e v_i, \\ C_{2q} &= 2\rho_{eq}v_e a_i \end{aligned} \qquad (i = u, d), \qquad (2.21)$$

where $\rho_{\nu e} \simeq \rho_{top} - 0.021$, and $\rho'_{\nu e} \simeq \rho_{top} - 0.0077$.

For the determination of the coefficients C_1, parity violating transitions in Cs are quite effective since for heavy nuclei the vector couplings of the quarks are coherently enhanced, in addition since Cs has only a single electron outside a completely filled shell, rather clean theoretical calculations for the atomic effects are available [53]. The results are expressed in terms of the weak charge $Q_W = -2(C_{1u}(2Z + N) + C_{1d}(Z + 2N))$ whose value is [54] $Q_W(^{133}_{55}Cs) = -71.04 \pm 1.58 \pm 0.88$ (the second error comes from atomic theory). The particular combination $C_{2u} - \frac{1}{2}C_{2d}$ has been also measured in the SLAC polarized $e-D$ scattering experiment [55]. The values of the parity–violating coefficients listed in table II have been derived from the quoted value of Q_W, and from the results given in table 1 of ref. [55].

2.4 Physics at the Z–peak

The recent experiments performed at the LEP and SLC Z–factories have provided us with a set of high precision measurements that are very sensitive to the values of the fermion couplings to the Z–boson.

Besides the accurate determination of the value of the Z–mass, that together with α and G_μ completes the set of fundamental input parameters of the SM, also the total Z width and the partial decay widths into hadronic final states and into each of the three lepton flavours have been measured at LEP with very high precision. Less accurate results have been obtained also for the b and c partial widths.

The measurements of the different Γ_f's are sensitive to the particular combination of couplings $v_f^2 + a_f^2$, while the independent combination $v_f a_f/(v_f^2 + a_f^2)$ enters the expressions of the on–resonance forward–backward asymmetries A_f^{FB}, that have been measured for $f = e, \mu, \tau, c, b$, and of the τ polarization asymmetry A_τ^{pol}.

i) Z decay widths

All the four LEP collaborations have measured the total Z–width Γ_Z as well as the hadronic and the three flavour–dependent leptonic partial widths Γ_h, Γ_e, Γ_μ and Γ_τ [33].

Due to the very high experimental accuracy, radiative corrections have to be carefully taken into account in all the theoretical expressions. At 1–loop, the partial decay width of the Z–boson to f–flavour fermions reads [36]

$$\Gamma_{Z\to f\bar{f}} = N_c^f \frac{M_Z}{12\pi}\sqrt{2}G_\mu M_Z^2 \rho_f (a_f^2 + v_f^2)(1 + \delta_{QED}^f)(1 + \delta_{QCD}^f), \qquad (2.22)$$

where $N_c^f = 3(1)$ for quarks (leptons). δ^f_{QCD} is the gluonic correction for hadronic final states ($\delta^f_{QCD} \simeq \alpha_s(M_Z^2)/\pi$ in leading order). For the strong coupling constant we have used the value $\alpha_s(M_Z^2) = 0.118 \pm 0.008$ determined from jet analysis in hadronic Z decays [56], and we have neglected the theoretical uncertainty related to the error on this parameter. δ^f_{QED} is a (small) additional photonic correction. Electroweak corrections appear in the ρ_f term as well as in the effective weak mixing angle that renormalizes the vector-coupling v_f :

$$\rho_f = \rho + \Delta\rho_f^{rem},$$
$$s^2_{eff}(f) = \frac{1}{2}\left[1 - \sqrt{1 - \frac{4\mathcal{A}}{\rho M_Z^2}\left(\frac{1}{1-\Delta\alpha} + \Delta\bar{r}_f^{rem}\right)}\right] \tag{2.23}$$
$$v_f = t_3^f - 2Q^f s^2_{eff}(f).$$

In these equations the ρ–term is universal and includes the potentially large heavy–top effects. $\Delta\rho_f^{rem}$ and $\Delta\bar{r}_f^{rem}$ contain, among others, non universal flavour–dependent contributions arising from vertex form factors. These contributions are generally small, except in the case of b–quarks final states for which loops involving the top–quark appear in the correction to the Zbb vertex [57]. Finite mass effects not displayed in eq. (2.22) have been also taken into account in the fit to the top mass of this chapter, as well as in the fit of chapter 4 to exotic fermions mixing. Analytical formulae for these corrections can be found in [36].

The experimental values of the five width Γ_Z, Γ_h, Γ_ℓ ($\ell = e, \mu, \tau$) as measured by the four LEP collaborations are affected by common systematic errors. For the weighted averages listed in table III we have assigned to Γ_Z a common systematic error of 5 MeV from point–to–point error in the LEP energy calibration, and to the partial widths a 0.5% error from luminosity [58]. Experimentally the widths are determined by fitting simultaneously the data for the reactions $e^+e^- \to hadrons$, e^+e^-, $\mu^+\mu^-$, $\tau^+\tau^-$, and thus they are expected to have correlations that cannot be neglected, but that unfortunately are not always given. To overcome this inconvenience, we have adopted the following procedure. A second set of experimental quantities equivalent to $\{ \Gamma_Z, \Gamma_h, \Gamma_e, \Gamma_\mu, \Gamma_\tau \}$, but with much cleaner correlations, is provided by $\{ \Gamma_Z, \sigma_h^0, R_e, R_\mu, R_\tau \}$ where σ_h^0 is the peak hadronic cross section corrected for the effect of initial state radiation, and $R_l = \sigma_h^0/\sigma_l^0 = \Gamma_h/\Gamma_l$ $(l = e, \mu, \tau)$. The correspondence between the two sets is given by

$$\sigma_f^0 = \frac{12\pi}{M_Z^2}\frac{\Gamma_e\Gamma_f}{\Gamma_Z^2}. \qquad (2.24)$$

A remarkable property of this second set of quantities is that their systematic errors have in general different origins and that the correlation arising from their functional relation to the measured observables is negligible, with the exception of the one between Γ_Z and σ_h^0. In order to make a definite ansatz we have assumed an anticorrelation between these two quantities of –25%. The correlation matrix for the set of widths, shown in table III, has been worked out via an iterative procedure by requiring that it reproduces this anticorrelation (together with vanishing small off–diagonal coefficients for the other entries) when we transform to the second set by means of eq. (2.24). We have explicitly checked that this procedure leads to quite acceptable results when confronted with the available correlations [33]

A direct measurement of the Z invisible width by single photon counting [59] $\Gamma_{\rm inv} = 500 \pm 76$ MeV has also been included in our analysis.

ii) Leptonic asymmetries.

Forward–backward asymmetries are defined as follows

$$A_f^{\mathrm{FB}} \equiv \frac{\sigma_F - \sigma_B}{\sigma_F + \sigma_B}, \qquad (2.25)$$

where σ_F (σ_B) is the cross section for events with the f- fermion scattered into the forward (backward) hemisphere with respect to the electron beam direction.

On resonance this gives

$$A_f^{\mathrm{FB}} = 3\,\frac{v_e a_e}{v_e^2 + a_e^2}\,\frac{v_f a_f}{v_f^2 + a_f^2}, \qquad (2.26)$$

where again $v_{e,f}$ should be expressed in terms of the effective weak mixing–angle (2.23). For quarks, final state QCD corrections must also be included (see *e.g.*[60]). It is important to notice that, while the values for the Z decay rates given by the experimental collaborations are the purely *'weak'* rates, i.e. they take into account the large QED corrections, this is usually not true for the given experimental FB asymmetries. This means that the experimental numbers should be not compared directly to eq. (2.26), but to the QED corrected expression, which can be obtained by convolving the $e^+e^- \to f\bar{f}$ differential cross sections with a suitable "radiator" kernel [61] (this allows to take into account the bulk of QED initial–state radiation, that are known to yield large corrections). The convoluted complete s-dependent formulae [61] (instead of just eq. (2.26)) has then be used to fit the asymmetries, both for the fit to m_t of section 5 and for the FIT of chapter 4.

Even if statistical errors are still large if compared with the uncertainties on the leptonic partial widths, the leptonic FB asymmetries constitute an additional important set of quantities for testing universality of the lepton couplings to the

Z. In fact, while the Γ_ℓ's are mainly sensitive to the squared axial couplings, the asymmetries are sensitive to the ratios v_ℓ/a_ℓ. The combined measurement of these two sets of quantities allows for an independent determination of v_ℓ and a_ℓ. In table III we give the values of the peak asymmetries averaged over the results of the LEP collaborations. Whenever available we have used the asymmetries determined from a maximum likelihood fit to the angular distribution $d\sigma_f/d\cos\theta \sim 1+\cos^2\theta + \frac{8}{3}A_f^{\rm FB}\cos\theta$ (where θ is the scattering angle), otherwise we have used the direct countings of the events and we have corrected for the relevant angular range of detection in the theoretical expressions.

The τ polarization asymmetry [62] has been also measured at LEP in τ pair production, using the distributions of its decay products [63]. At the Z resonance this quantity reads

$$A_\tau^{pol} = \frac{-2v_\tau a_\tau}{v_\tau^2 + a_\tau^2} \tag{2.27}$$

and it is very sensitive to the τ vector coupling to the Z, having the advantage with respect to the forward–backward asymmetry that it is not suppressed by the small electron vector coupling. Experimentally, the τ polarization is inferred from the slope of the energy distribution of the decay products under the assumption of pure V − A coupling with the $W^\pm$ bosons [62]. The weighted average of the ALEPH and OPAL results [63] is given in table III.

iii) Heavy flavours

For the measurement of the width of the Z decay into b quarks, different methods have been used by different collaborations. ALEPH, L3 and OPAL at LEP and MARK II at SLC [64] used high momentum and high–$p_{\rm T}$ muons and/or electrons to tag the b quark, thus they measure the quantity $\Gamma_b/\Gamma_h\, Br(b\to \ell\nu X)$

TABLE III. Results on Z–partial widths (in MeV) and on–resonance asymmetries. The values displayed for the leptonic asymmetries correspond to the peak–data and have been corrected only for angular acceptance. Also displayed are the values of the b and c axial–vector couplings extracted from the off–resonance $A^{\gamma Z}_{b,c}$ asymmetries (where each one is obtained fixing the other to the SM value) and the charm asymmetry measured only through D^*–tagging (independently on assumptions on the b–quark couplings.

Quantity	Experimental value	Correlation			
Γ_Z	2487 ± 10	0.52	0.52	0.29	0.25
Γ_h	1739 ± 13		–0.15	0.55	0.48
Γ_e	83.2 ± 0.6			–0.08	-0.07
Γ_μ	83.4 ± 0.9				0.26
Γ_τ	82.8 ± 1.1				
$A_e^{\mathrm{FB}}(peak)$	-0.019 ± 0.014				
$A_\mu^{\mathrm{FB}}(peak)$	0.0070 ± 0.0079				
$A_\tau^{\mathrm{FB}}(peak)$	0.099 ± 0.096				
A_τ^{pol}	-0.121 ± 0.040				
Γ_b	367 ± 19				
Γ_c	299 ± 45				
A_b^{FB}	0.123 ± 0.024				
A_c^{FB}	0.064 ± 0.049				
$a_b^{\gamma Z}$	-0.405 ± 0.095				
$a_c^{\gamma Z}$	0.515 ± 0.085				
$A^{\gamma Z}_{c,D^*}$ (29 GeV)	-0.101 ± 0.027				
$A^{\gamma Z}_{c,D^*}$ (35 GeV)	-0.161 ± 0.034				

for $\ell = e, \mu$. A value for the b–branching ratio into electrons and muons is then needed for the determination of Γ_b. This branching has been measured by the L3 collaboration [65] by analysing the ratio of the events where both b's decay semileptonically to the single lepton events. The L3 measurement can be combined with the PEP and PETRA determination of $Br(b \to \ell\nu X)$ (quoted in [65]) to obtain a value that is largely independent of assumptions on the b neutral–current couplings since the first result is, in first order, independent of Γ_b, and at the c.m. energies of the latter experiments weak effects contribute only a few percent to b–production. We have used the resulting value $Br(b \to \ell\nu X) = 0.119 \pm 0.006$ [65] for deriving Γ_b/Γ_h from the average of the first four measurements. The strategy adopted by DELPHI [64] in order to identify the b quarks is based on the fact that, due to the larger B–hadrons mass, a greater "sphericity" is expected for the corresponding jets. This measurement gives a further direct determination of the Γ_b/Γ_h ratio.

From the overall average of these quantities and using the experimental value of Γ_h (table III), we obtain $\Gamma_b = 363 \pm 19$ MeV, where the overall uncertainty is dominated by the error on the b–semileptonic branching ratio.

The Z partial decay width into charmed quarks has also been measured, but due to the greater difficulties in the identification of the primary c quarks the accuracy achieved is worse. ALEPH [66] uses high p and p_{T} electrons while OPAL uses muons [66]. Averaging these two measurements and using the value $Br(c \to \ell\nu X) = 0.096 \pm 0.006$ determined at PEP and PETRA and quoted by L3 in [65] a first value for Γ_c/Γ_h is obtained.

A second determination of the $c\bar{c}$ production rate has been performed by OPAL (last paper in [66]) with a different method. The Γ_c/Γ_h ratio is determined from the analysis of the reconstructed D^* momentum distribution produced in Z decays. The same ratio has been determined by the DELPHI collaboration [66] from the inclusive analysis of charged pions from $D^{*+} \to \pi^+ D^0$ decay. In combining these two measurements, the common systematic error coming from the $c \to D^*$ hadronization probability has been taken into account. The result of the average of the four measurement is given in table III.

Three measurements of the b–quark forward–backward asymmetry have been reported [67]. In each case the b channel is selected using electronic and muonic b decays, with the requirement of high p and $p_{\rm T}$ for the final leptons, the consequent reduction in the statistics leads to rather large experimental errors. In addition the effect of $B^0 - \bar{B}^0$ mixing has to be taken into account. This effect tends to reduce the asymmetry since the neutral B^0 meson can transform into its charge conjugate before it decays. The relation between $A_b^{\rm FB}$ and the *observed* asymmetry is [68]

$$A_b^{\rm FB} = \frac{A_{obs}^{\rm FB}}{1 - 2\chi_B}, \tag{2.28}$$

where χ_B is a measure of the probability of a B^0 meson to oscillate into a $\bar{B}^0$ meson. Several measurements of the B–mixing parameter have been performed [69]. The method adopted, which is largely independent of the b–quark neutral couplings, is to count the ratio between like–sign to opposite–sign b–originated di–lepton events, since two leptons of the same charge are a signature that one B^0 meson has oscillated into its CP conjugate.

The result quoted in table III for the b forward–backward asymmetry has been obtained by adjusting all the measurements to $\chi_B = 0$, and then correcting the average with $\chi_B = 0.146 \pm 0.016$ that was obtained by averaging the ALEPH, L3 and UA1 measurements [69]. [7]

The forward–backward asymmetry for charmed quarks has been measured only by the ALEPH collaboration [67] in a simultaneous fit with $A_b^{\rm FB}$. Their result is displayed in Tab. III.

We have included in our analyses also the FB b and c asymmetries $A_{b,c}^{\gamma Z}$, measured in the γ–Z interference region at PEP and PETRA. These asymmetries are essentially determined by the product of the axial–vector couplings $a_e a_{b(c)}$, that is a different combination from what is measured on top of the resonance. High p and p_T leptons have been used for tagging both the heavy quarks [71,72], leading to non negligible correlations between the two asymmetries. For the c quark also the D^* tagging technique (largely independent of the b couplings) have been used [73,72]

The measurements of the leptonic asymmetries in weak–electromagnetic interference could also be used to constrain the leptonic couplings, however they turn out to be much less important than the constraints for these couplings that we have discussed, so they have not been included in our fits.

[7] We have not included the ARGUS and CLEO results [70] since these observations stem from the analysis of $\Upsilon(4S)$ decays were only B_d mesons are produced, while at LEP the relative abundance of B_s to B_d mesons is estimated to be of 0.3-0.4.

2.5 Result of the fit to the top mass

The experimental constraints introduced in the previuos sections can be used to fit the top mass in the SM. The top–quark enters the theoretical expressions through the loop effects, as we have discussed. We have minimized the χ^2 function with these constraints, using the MINUIT program. In this fit we have not used the universality constraint in the lepton sector, which would have allowed to use a more precise Γ_l measurement of LEP, instead of the flavor dependent rates Γ_e, Γ_μ and Γ_τ. In this way, we obtain a sligtly less stringent range for m_t than we would get in the pure SM. On the other hand, we recall that our main aim (see chapter 4) is to fit models which extend the SM and do not present light leptons universality.

Fixing the Higgs mass at $m_H = 100$ GeV and the strong coupling constant at the value $\alpha_s = 0.118 \pm 0.008$ determined from jet analysis, we obtain the result, $m_t = 116^{+28}_{-35}$ GeV ($m_t < 166$ GeV at 95 % confidence level), consistent with the dedicated analyses of ref. [74]. Just as an exercice, we have also fitted the value of the strong coupling constant in the SM, fixing the top mass obtaining $\alpha_s = 0.123 \pm 0.012$, in agreement with the above value extracted for jet analyses.

Chapter 3

Mixing between ordinary and exotic fermions

The lack of observation of new particles in the last accelerator runs indicates that if possible new fermions exist, they will generally have large masses ($> 50-100$ GeV). Even if these particles cannot be directly produced with the experimental facilities available at present, it is still possible that their effects are indirectly detected as small deviations of the observed fermion couplings from the standard ones. In particular, this happens if the exotic fermions have non–canonical $SU(2)_L \times U(1)$ assignments and they mix with the ordinary ones. We consider a fermion to have canonical $SU(2)_L$ quantum numbers if it is a left–handed $SU(2)_L$ doublet or a right–handed $SU(2)_L$ singlet. These are called ordinary fermions while fermions with non–canonical quantum numbers are classified as exotics. Exotic fermions can appear in mirror models [75] in which generally whole mirror generations with R–doublets and L–singlets are introduced, in models with vector doublets (singlets) where both left and right fermions have the same transformation properties under weak–isospin, or as singlet Weyl neutrinos. Fermions with exotic charges or colour assignments cannot mix with the known quarks and leptons and thus we will not consider them.

Theoretically, in most models the mixings arise together with the symmetry breaking phenomena which lead to the generation of masses. Natural ways to get the large mass splittings between the ordinary light fermions and the exotic heavy ones are provided by the 'see–saw' mechanisms. In the 'quadratic' see–saw the mixing angle θ between a light fermion of mass m and an heavy fermion of mass M is typically $\sin^2\theta \sim (m/M)^2$. In the 'linear' see–saw, the relation is $\sin^2\theta \sim m/M$. We see then that the mixings of the 3$^{\rm rd}$ generation are naturally expected to be the large ones. In the next chapter, we will analyze the phenomenological consequences of the mixing, obtaining the bounds on the mixing angles from a fit with all the the experimental constraints discussed in the previous chapter [31]. In particular, the recent experimental results from Z–peak measurements stringently constrain most of the mixings, including the expected large ones of the 3$^{\rm rd}$ generation [76,31].

The model–independent formalism for the description of fermion mixing, independently from the mechanism by which it is generated, was introduced in ref. [47] and will be presented in this chapter following ref. [31]. We will define the formalism for the description of mixing for the charged fermions sector in section 1, and for the neutral fermions sector in section 2.

3.1 Charged fermions

In order to describe the mixing between ordinary and exotic charged fermions, we introduce [47,31] two vectors for the left and right–handed ordinary and exotic weak eigenstates $\Psi^o_{L(R)} = (\Psi^o_O, \Psi^o_E)^T_{L(R)}$, and two different vectors for the light and heavy mass eigenstates $\Psi_{L(R)} = (\Psi_l, \Psi_h)^T_{L(R)}$. The weak and mass eigenstates are related by unitary transformations

$$\Psi^o_{L(R)} = U_{L(R)} \Psi_{L(R)}. \tag{3.1}$$

It is convenient to decompose the matrix U as

$$U_{L(R)} = \begin{pmatrix} A & E \\ F & G \end{pmatrix}_{L(R)}, \tag{3.2}$$

where A and F describe the overlap of the light eigenstates with the ordinary and exotic fermions respectively. Since we have included fermions of sequential families or canonical members of vector multiplets as ordinary states, the labels 'light' and 'heavy' should be taken as suggestive only. From the unitarity of U it follows that

$$A^\dagger A + F^\dagger F = AA^\dagger + EE^\dagger = I. \tag{3.3}$$

Hence, the matrix A describing the mixing with the ordinary fermions is non–unitary by small terms quadratic in the ordinary–exotic fermion mixings present in F.

The fermion current coupling to the Z is

$$\frac{1}{2} J^\mu_Z = \sum_f \bar{\Psi}^o_f \gamma_\mu (t^f_3 I_L P_L + t^f_3 I_R P_R - Q^f s^2_W I) \Psi^o_f, \tag{3.4}$$

where $P_{L,R} = \frac{1}{2}(1 \mp \gamma_5)$ are the L and R chiral projectors, $s^2_W \equiv \sin^2\theta_W$, Q^f and t^f_3 denote charge and third isospin component of f and $I_{L,R}$ project onto the subspaces of the ordinary and exotic weak doublets of Ψ^o, *i.e.*

$$I_L = \begin{pmatrix} I & 0 \\ 0 & 0 \end{pmatrix} \quad , \quad I_R = \begin{pmatrix} 0 & 0 \\ 0 & I \end{pmatrix}. \tag{3.5}$$

Hence, (omitting the label l) the light fermions–Z vertex is given by the Lagrangian

$$\mathcal{L}_Z = -\left(\sqrt{2} G_F M^2_Z\right)^{1/2} \sum_f \bar{\Psi}_f \gamma_\mu (L^f P_L + R^f P_R) \Psi_f \; Z^\mu, \tag{3.6}$$

with

$$L^f = t_3^f A_L^{f\dagger} A_L^f - Q^f s_W^2$$
$$R^f = t_3^f F_R^{f\dagger} F_R^f - Q^f s_W^2. \tag{3.7}$$

Although the matrices $A^\dagger A$ and $F^\dagger F$ are in principle quite general, non–vanishing off diagonal terms would induce FCNC that are experimentally known to be very suppressed [47]. Hence, we will assume that different light mass eigenstates do not mix with the same exotic partner, in which case the absence of FCNC is automatically guaranteed. With this assumption one gets

$$(F_a^\dagger F_a)_{ij} = (s_a^i)^2 \; \delta_{ij} \; , \qquad a = L, R, \tag{3.8}$$

where $(s_a^i)^2 \equiv 1 - (c_a^i)^2 \equiv \sin^2\theta_a^i$, and $\theta_{L(R)}^i$ is the mixing angle between L(R) light and heavy partners.

Then the neutral–current couplings for the light fermions can be written as

$$\hat{\epsilon}_L(f_i) \equiv (L^f)_{ii} = t_3^{f_i}(c_L^{f_i})^2 - Q^{f_i} s_W^2$$
$$\hat{\epsilon}_R(f_i) \equiv (R^f)_{ii} = t_3^{f_i}(s_R^{f_i})^2 - Q^{f_i} s_W^2, \tag{3.9}$$

and we see that while the L–mixings reduce the strength of the isospin current, the presence of R–mixings induces a right–handed current. Clearly the electromagnetic current is left unchanged. The vector and axial–vector couplings in the presence of mixing are (omitting the generation index i)

$$v_f \equiv \hat{\epsilon}_L(f) + \hat{\epsilon}_R(f) = t_3^f \left[(c_L^f)^2 + (s_R^f)^2\right] - 2Q^f s_W^2$$
$$a_f \equiv \hat{\epsilon}_L(f) - \hat{\epsilon}_R(f) = t_3^f \left[(c_L^f)^2 - (s_R^f)^2\right]. \tag{3.10}$$

Henceforth v_f and a_f will always denote the true couplings of the light fermions including mixing terms.

The charged current between light states is

$$\frac{1}{2}J^\mu_W = \bar{\Psi}_u\gamma^\mu(V_L P_L + V_R P_R)\Psi_d. \tag{3.11}$$

The first 3 components of the vectors Ψ_u, Ψ_d represent the standard quarks, while the remaining $n-3$ 'light' fields correspond to possible extra sequential, or vector doublet, quarks. $V_L = A_L^{u\dagger}A_L^d$ and $V_R = F_R^{u\dagger}F_R^d$ generalize the SM Cabibbo-Kobayashi-Maskawa (CKM) quark mixing. In particular, the matrix V_L is non unitary due to the mixing with the exotic quarks, however it can be decomposed as

$$V_{L\,ij} = c_L^{u_i} c_L^{d_j} K_{L\,ij}, \tag{3.12}$$

where K_L is unitary [47]. For the induced right–handed currents, it is convenient to introduce the parameters

$$\kappa_{ij} \equiv \frac{V_{R\,ij}}{K_{L\,ij}}, \tag{3.13}$$

which are quadratic in the light–heavy mixings.

3.2 Neutral fermions

For the neutral fermions the situation is more complicated because in the presence of Majorana mass terms three kinds of neutral fields with different isospin assignments can mix at the same time, and also because due to the lack of experimental constraints the assumption on the absence of FCNC must be released. Besides the ordinary neutrinos that appear in L–doublets $(n_O^o,\ e_O^{o-})^T$, we can have exotic states that appear in the CP conjugates of $SU(2)$ R-doublets $(E_E^{o+} n_E^o)_L^T$, (these can mix with n_O^o through $\Delta \mathrm{L} = \pm 2$ Majorana mass terms) and also exotic singlets n_{SL}^o can be present.

In analogy with the charged fermion case, we write the weak and mass eigenstates as

$$n_L^o = \begin{pmatrix} n_O^o \\ n_E^o \\ n_S^o \end{pmatrix}_L \quad , \quad n_L = \begin{pmatrix} n_l \\ n_h \end{pmatrix}_L . \tag{3.14}$$

These states are related through $n_L^o = U_L n_L$. The unitary matrix U can be decomposed as

$$U_L = \begin{pmatrix} A & E \\ F & G \\ H & J \end{pmatrix}_L , \tag{3.15}$$

with A, F, H describing the overlap of the light neutrinos with n_O^o, n_E^o and n_S^o respectively.

Note that we do not distinguish between left handed neutrinos and antineutrinos, they are all described by fields n_L and the right handed fields will be denoted as $n_R^c = C\bar{n}_L^T$. Clearly $n_R^{oc} = U_R n_R^c$ with $U_R = U_L^*$.

The LEP measurements of the number of light neutrino species implies that if neutrinos with large exotic n_E^o components exist, their masses must be heavier than $M_Z/2$. Light singlets, however, as in the case of Dirac neutrino masses, could be present and a mixing with exotic doublets would allow them to couple to the Z boson. For simplicity we will not consider this case, but our results are largely independent of this restriction. In conclusion we will assume the light neutrinos to be mainly ordinary states so that we will consider the elements of F and H as small light–heavy mixings.

We will chose the flavour basis such that the charged lepton flavour eigenstates coincide with the charged mass eigenstates up to light–heavy mixing effects. Hence, the charged current between light mass eigenstates reads

$$J^{\mu}_{W} = \bar{n}_L \gamma^{\mu} A_L^{\nu\dagger} c_L^e e_L + \bar{n}_R^c \gamma^{\mu} F_R^{\nu\dagger} s_R^e e_R. \tag{3.16}$$

The first term in this equation is the usual left–handed current with the overall strength reduced by the effect of light–heavy mixing, while the second term corresponds to an induced right–handed current that can produce neutrinos of the wrong helicity in weak decays. This term is present when both the light neutrino and charged lepton mix with the components of an exotic doublet.

It is convenient to write $A^{\nu\dagger} = K^{\nu}\mathcal{A}^{\nu\dagger}$, where the matrix K^{ν} is unitary and, being the leptonic analog of the CKM matrix, it is non–trivial if the light neutrinos have masses and ordinary mixings. The exotic mixings appear only in $\mathcal{A}$, which deviates from the identity only by terms of $O(s^2)$. In the charged current processes that we will consider, a sum has to be taken over the unobserved final neutrino mass eigenstates (the kinematical effects of ν masses are negligible) and thus the information in K^{ν} is lost. In weak decays, for example, the mixings induce a change in the decay rate with respect to the SM rate Γ_o that, to $O(s^2)$ and restricting ourself to the primary vertex, can be written as

$$\frac{1}{\Gamma_o}\sum_i \Gamma(e_a \to n_i) = (c_L^{e_a})^2 (A_L^{\nu} A_L^{\nu\dagger})_{aa} + O(s^4), \tag{3.17}$$

where $(A^{\nu}A^{\nu\dagger})_{aa} = (\mathcal{A}^{\nu}\mathcal{A}^{\nu\dagger})_{aa} \equiv (c_L^{\nu_a})^2$ accounts for the neutrino light-heavy mixing. As we see, the sum over the final undetected states allows us to take just one mixing angle per neutrino flavour to describe the exotic mixings, although in general the matrix $\mathcal{A}^{\nu\dagger}\mathcal{A}^{\nu}$ is not diagonal.

The weak neutral current for the light neutrino states is

$$J^{\mu}_{\nu Z} = \frac{1}{2}\bar{n}_L \gamma^{\mu} (A_L^{\nu\dagger} A_L^{\nu} - F_L^{\nu\dagger} F_L^{\nu}) n_L, \tag{3.18}$$

where $A_L^{\nu\dagger} A_L^{\nu}$ and $F_L^{\nu\dagger} F_L^{\nu}$ originate respectively from the ordinary n_O^o and exotic n_E^o neutrinos that have opposite isospin assignments.

Up to mixing effects in the target, and summing again over the undetected light n_i neutrinos, the scattering process $n_a \to n_i$ is modified with respect to the normal case as

$$\begin{aligned}\frac{1}{\sigma_o}\sum_i \sigma(n_a \to n_i) &= \frac{1}{(c_L^{\nu_a})^2}(A^\nu(A^{\nu\dagger}A^\nu - F^{\nu\dagger}F^\nu)^2 A^{\nu\dagger})_{aa} \\ &= 1 - 2\left(K^{\nu\dagger}(2F^{\nu\dagger}F^\nu + H^{\nu\dagger}H^\nu)K^\nu\right)_{aa} + O(s^4), \end{aligned} \tag{3.19}$$

where the factor $(c_L^{\nu_a})^2$ in the denominator comes from the normalization of the n_a produced in the weak decay of e_a. In (3.19) we have used the unitarity of U_L as well as the decomposition of the matrix A into the unitary K matrix, and we have neglected terms $O(s^4)$. Defining now $(K^\dagger F^\dagger F K)_{aa} \equiv \lambda_F^a (s_L^{\nu_a})^2$ and $(K^\dagger H^\dagger H K)_{aa} \equiv \lambda_H^a (s_L^{\nu_a})^2$ we finally get

$$\frac{1}{\sigma_o}\sum_i \sigma(n_a \to n_i) = 1 - \Lambda_a (s_L^{\nu_a})^2 + O(s^4). \tag{3.20}$$

Since the sum of the λ^a' s is constrained to be ≤ 1 from the unitarity of U_L in (3.15), the value of the effective parameter $\Lambda_a \equiv 4\lambda_F^a + 2\lambda_H^a$ must lie between 0 and 4, depending on the mixing involved. If the light states are mixed with ordinary states (that will be mainly heavy) then the couplings are not affected and $\Lambda_a = 0$. If only singlet states n_S^o mix with the known neutrinos then $\Lambda_a = 2$ while $\Lambda_a = 4$ describes mixings involving only exotic states n_E^o.

The decay rate of the Z boson into undetected neutrinos is proportional to the sum of the square of the neutrino neutral–current couplings. Using the same approximations as in the previous case we find

$$\mathrm{Tr}(A^{\nu\dagger}A^\nu - F^{\nu\dagger}F^\nu)^2 = 3 - \sum_a \Lambda_a (s_L^{\nu_a})^2 + O(s^4), \tag{3.21}$$

and we see that the effective parameter Λ_a could largely influence the reduction in the decay rate.

Chapter 4

Global analysis of fermion mixing with exotics

In the last few years the ever increasing accumulation of precise electroweak experiments have been regularly employed to check the consistency of the standard model (SM), to determine $\sin^2\theta_W$ and to make predictions for the still unknown value of the top mass. Possible indirect signatures of physics beyond the SM, such as the effects of additional gauge bosons or of mixings of the standard fermions with exotic ones, as well as the contributions of non–decoupled physics to radiative corrections, have also been constrained by these measurements.

The first pre–LEP analyses [77,78,47] used the available information on gauge boson masses from colliders, neutral current (NC) data on ν scattering, parity violation, fermion asymmetries in e^+e^- annihilation below the Z resonance, and in some cases charged current (CC) constraints. By now the situation has improved considerably. A remarkable improvement has been achieved in the determination of the W boson mass from UA2 and CDF [37]. In the NC sector, there are new measurements on atomic parity violation in Cs [54] and new calculations of the atomic matrix elements involved [53], there are new results on $\nu_\mu e$ scattering [51,50,52] as well as new and updated analyses of the c and b asymmetries in γ–

Z interference processes at PEP and PETRA [71,73,72]. In the CC sector, new constraints are available on the universality of the lepton couplings and on the unitarity of the quark mixing matrix, and the problem of the charm quark threshold [79], that affects the νq CC cross section used to normalize the deep-inelastic NC experiments, has been studied in more detail. The really new input, however, comes from the large set of accurate measurements carried out at the Z–peak at LEP and SLC. Besides M_Z, that is now very precisely known, the determination of the total and of the partial Z–widths and of the on–resonance forward–backward and τ polarization asymmetries has provided very precise informations about the fermion couplings to the Z.

Some of these data have been recently used to update the predictions on m_t [80] and to constrain extensions of the SM with extra U(1) gauge bosons [81], as well as technicolour models, strongly interacting Higgs–bosons and other kinds of heavy physics that could manifest itself through radiative corrections [82].

It is our purpose here to update the bounds on possible mixings between the known fermions and new exotic ones using this new set of data, which we have already presented in chapter 2. There have been several earlier analyses of the limits on fermion mixings [83], and the first (pre-LEP) global analysis of this kind of new physics was done by Langacker and London [47]. Subsequently, Nardi and Roulet [76] showed that the very first LEP data already improved some bounds significantly, more recently, Langacker, Luo and Mann [84] have also discussed the sensitivity to some exotic mixings that will be attained with the forseeable precision of the ongoing or planned precision electroweak experiments.

The existence of new fermions with exotic weak couplings is a quite common feature in most of the extensions of the SM, being the 'superstring inspired' E_6 models well known and still popular examples [85] of these. A mixing between ordinary and exotic fermions is allowed whenever their $\mathrm{SU}(3)_C \times \mathrm{U}(1)_{\mathrm{em}}$ quantum numbers are the same. If at the same time the new fermions have non canonical $SU(2)_L$ assignments, the couplings of the light states with both the W and the Z vector bosons will be modified, as we have seen in chapter 3, leading to deviations from the SM expectations. This is the kind of effects we aim to constrain by means of a careful analysis of the available experimental results.

The general formalism to describe fermion mixing that was introduced in [47] has been briefly surveyed in the previous chapter. Here we show in section 1 the modifications induced by mixings in the theoretical expressions for the different observables that we have used to work out the constraints, which were described in chapter 2. In section 2 we comment on the results of the global analysis [31]. The results are presented as 90 % c.l. upper limits on the ordinary–exotic mixing parameters, both in the case in which only one fermion is allowed to mix at a time ('single' fits), and in the case were all mixings are simultaneously present so that accidental cancellations may occur ('joint' fits). Finally, in section 3 we draw our conclusions.

4.1 How mixings modify theoretical expectations

In this section we discuss the effect of mixings in the set of experimental constraints introduced in chapter 2. In comparing the experimental results with the corresponding theoretical expressions some care is needed, since indirect effects of the mixings that depend on the particular experimental procedure used to extract the data could be present.

To match the precision reached by the 'last–generation' experiments, 1-loop effects should be taken into account in the evaluation of the theoretical expressions. We have followed the general attitude of including only the set of SM radiative corrections, which are nowadays completely known, neglecting the effect of mixings in them as well as the contribution of the additional states in the loops. We should stress however that the large number of exotic fermions present in the models under investigation could give rise to non negligible higher order effects [82] especially in the case of non-degenerate doublets [35]. QCD corrections have also been included in all the relevant cases when hadronic final states were involved.

Our set of fundamental input parameters consists of the QED coupling constant α measured at $q^2 = 0$, the mass of the Z boson M_Z and the Fermi coupling constant G_F. The numerical values of α and M_Z as extracted from experiments are not affected by the mixings. The position of the resonance–peak does not depend on the exact form of the fermion couplings with the Z (the shape and height of the peak, in contrast, are modified by the mixings) and the standard set of QED corrections needed to reconstruct the exact peak–position can be safely applied, since also the electromagnetic current is not modified.

In contrast with the previous two parameters, the Fermi coupling constant extracted from the measured life–time of the μ-lepton, $G_\mu = 1.16637(2) \times 10^{-5}\text{GeV}^{-2}$, is affected by fermion mixings. The relation between G_F and the effective μ-decay coupling constant (neglecting the $O(s^4)$ effect of induced right handed currents (RHC)) is

$$G_\mu = G_F c_L^{\nu_e} c_L^{\nu_\mu} c_L^e c_L^\mu. \qquad (4.1)$$

Clearly, this indirect dependence on the light lepton mixing angles is propagated in all the expressions that contain G_F. This is the case for example for the W boson mass, for which no other explicit dependence on mixings appears.

In addition, also the value of the top-quark m_t and Higgs boson M_H masses must be specified, since they enter the expressions via loop corrections. The dependence on M_H is soft, and we keep its value fixed at 100 GeV. In contrast, varying the value of m_t can induce sizeable effects. We have chosen to fix the top mass at the value $m_t = 120$ GeV that corresponds approximately to the minimum of our χ^2 function when all the mixing parameters are set to zero, as we have anticipated in chapter 2.

Whenever some other experimental parameter enters our theoretical expressions, we have used those experimental determinations for which mixing effects are absent or negligible. This will be the case *e.g.* of the strong coupling constant $\alpha_s(M_Z^2)$, of the semileptonic branching ratio $Br(b \to \ell + X)$ and of the $B^0 - \bar{B}^0$ mixing parameter χ_B on which we have commented in chapter 2.

The W mass

According to eq. (2.4) which holds in the SM, taking into account that the mixings affect the Fermi coupling constant as in eq. (4.1), the theoretical expression for the W mass reads

$$M_W^2 = \frac{\rho M_Z^2}{2}\left[1 + \sqrt{1 - \frac{G_\mu}{G_F}\frac{4\mathcal{A}}{\rho M_Z^2}\left(\frac{1}{1-\Delta\alpha} + \Delta r^{rem}\right)}\,\right], \qquad (4.2)$$

where $\mathcal{A} = \pi\alpha/\sqrt{2}G_\mu$ as before.

The expression for M_W in (4.2) is affected by the mixings only indirectly via the G_μ/G_F ratio. We note that increasing values of both the mixing angles and of the top mass (through ρ) tend to increase M_W. Since the same interdependence enters also the expression for the effective weak–mixing angle that defines the neutral–current couplings of the fermions, a sizeable anticorrelation between m_t and the light lepton mixings is to be expected, resulting into a stronger constrain for larger values of m_t.

Charged currents

i) Lepton universality

The ratios g_μ/g_e and g_τ/g_e of the leptonic couplings to the W boson are modified by fermion mixings according to

$$\left(\frac{g_i}{g_e}\right)^2 = \frac{(c_L^{l_i})^2(c_L^{\nu_i})^2 + (s_R^{l_i})^2(s_R^{\nu_i})^2}{(c_L^e)^2(c_L^{\nu_e})^2 + (s_R^e)^2(s_R^{\nu_e})^2} \simeq \frac{(c_L^{l_i})^2(c_L^{\nu_i})^2}{(c_L^e)^2(c_L^{\nu_e})^2}, \qquad i = \mu, \tau. \tag{4.3}$$

ii) CKM unitarity

Fermion mixings lead to violations of the 3-generation unitarity of the observable CKM matrix V_{ij}, $(i,j = 1,2,3)$, as is apparent from eq. (3.11–3.13). Thus, a measurement of the deviation from unity of the sum of the $|V_{ij}|^2$, for each matrix row, puts constraints on the mixings. As we have discussed in chapter 2, V_{ud} and V_{us} are obtained by dividing by G_μ the measured vector coupling in β decay and in K_{e3} and hyperon decays, respectively. Hence [47],

$$V_{ui} = \frac{G_F}{G_\mu}(V_{L\,ui} + V_{R\,ui})c_L^e c_L^{\nu_e}, \qquad i = d, s. \tag{4.4}$$

The value of $|V_{ub}|$, obtained from the analysis of semileptonic B decays, is negligibly small for our purposes. Using the unitarity of the matrix K_L introduced in (3.12), and neglecting terms of $O(s^4)$ and $O(s^2 \sum_{i=4}^{n} |K_{L\,ui}|^2)$,

$$\sum_{i=1}^{3} |V_{ui}|^2 = \left(\frac{G_F}{G_\mu} c_L^e c_L^{\nu_e}\right)^2 \Big\{ (c_L^u)^2 - \sum_{i=4}^{n} |K_{L\,ui}|^2 + \sum_{i=1}^{2} |V_{ui}|^2 \left[2\mathrm{Re}(\kappa_{ui}) - (s_L^{d_i})^2\right] \Big\}, \tag{4.5}$$

where we have approximated $|K_{L\,ui}|^2$ with the experimental values $|V_{ui}|^2$ in the coefficients of the $O(s^2)$ terms.

In chapter 2 we have also seen that V_{cd} is determined from the di-muon production rate of charm off valence d-quarks [45] while V_{cs} is extracted from D_{e3} decays [23]. Hence

$$|V_{cd}|^2 \simeq (c_L^c)^2 |K_{L\,cd}|^2, \qquad |V_{cs}|^2 \simeq |K_{L\,cs}|^2 [(c_L^c)^2 (c_L^s)^2 + 2\mathrm{Re}(\kappa_{cs})] \tag{4.6}$$

where, due to the comparatively large uncertainty affecting these measurements, those mixings that are more effectively constrained by other experiments have been neglected. Taking the sum, and neglecting also $|V_{cb}|^2$ and $O(s^4)$ terms, we obtain

$$\sum_{i=1}^{3} |V_{ci}|^2 \simeq (c_L^c)^2 - \sum_{i=4}^{n} |K_{L\,ci}|^2 + [2\mathrm{Re}(\kappa_{cs}) - (s_L^s)^2] |V_{cs}|^2. \tag{4.7}$$

iii) Right handed currents

The RHC's induced by mixings with exotic quarks allow to constrain directly the κ_{ij} parameters of the hadronic sector, as we have seen in chapter 2.

The leptonic RHC's are limited by the measurements of the μ and τ Michel parameters, as well as by the electron polarization in β decays. The corresponding bounds on parameters such as $s_R^{e_a} s_R^{\nu_a}$ have not improved with respect to those obtained in [47], so we will not repeat them here.

Neutral currents

The effect of fermion mixing in NC observables can be accounted for by some G_F/G_μ factor and by modifying eq. (2.14) according to eq. (3.10), i.e.

$$\begin{aligned} v_f^i \equiv \hat{\epsilon}_L(f) + \hat{\epsilon}_R(f) &= t_3^f \left[(c_L^f)^2 + (s_R^f)^2 \right] - 2Q^f k_i s_W^2 \\ a_f \equiv \hat{\epsilon}_L(f) - \hat{\epsilon}_R(f) &= t_3^f \left[(c_L^f)^2 - (s_R^f)^2 \right] . \end{aligned} \tag{4.8}$$

There are then effects induced by the normalisation procedures of the different experiments, as we are going to discuss now.

i) Neutrino – quark sector

In comparing the experimental results of chapter 2, section 3, with the theoretical expressions, the effect of the mixings in the normalization factors has to be taken into account as well [47], since the fermion charged–current couplings are modified according to (3.11) and, as discussed in the previous subsection, also the value of the CKM element V_{ud} obtained from β-decay experiments is affected.

Using now (3.6), (3.10) and (3.20) and taking the normalization effects properly into account, the values of the quark couplings as extracted from experiments correspond to

$$\epsilon_{L,R}(q) = \frac{1}{2} N_1(s^2, \kappa) \left[\left(1 - \Lambda_\mu (s_L^{\nu_\mu})^2/2\right)(v_q \pm a_q) + \lambda_{qL,R} \right], \tag{4.9}$$

where

$$N_1(s^2, \kappa) = \frac{1}{1 - (s_L^\mu)^2 - (s_L^{\nu_\mu})^2 - \mathrm{Re}(\kappa_{ud})}. \tag{4.10}$$

ii) Neutrino - electron sector

The electron vector and axial–vector couplings are extracted from $\nu_\mu - e$ scattering experiments that, as in the previous case, are normalized with the ν_μ-hadron charged–current cross sections. For high–energy neutrinos like those of CERN and FERMILAB, the CC deep–inelastic process leads to the same normalization factor as in the $\nu - q$ sector, so that the relation between the couplings extracted from experiments and the theoretical ones is

$$g_V^e = N_1\left(1 - \Lambda_\mu (s_L^{\nu_\mu})^2/2\right) v_e \qquad , \qquad g_A^e = N_1\left(1 - \Lambda_\mu (s_L^{\nu_\mu})^2/2\right) a_e. \tag{4.11}$$

For the low-energy neutrinos of BNL, the CC scattering is a quasi–elastic process so that the factor $N_1(s^2,\kappa)$ in eq. (4.11) is replaced by [47]

$$N_2(s^2) = \frac{1}{1 - (s_L^\mu)^2 - (s_L^{\nu_\mu})^2}. \tag{4.12}$$

iii) Electron - quark sector

iii) The effect of mixing here is again to modify the axial and vector couplings in eq. (2.21); a factor G_F/G_μ appears also for normalisation with muon decay. Hence

$$\begin{aligned} C_{1q} &= 2\left(\frac{G_F}{G_\mu}\right)\rho'_{eq} a_e v_i, \\ C_{2q} &= 2\left(\frac{G_F}{G_\mu}\right)\rho_{eq} v_e a_i \end{aligned} \qquad (i = u, d), \tag{4.13}$$

Physics at the Z–peak

Already the first experimental results of LEP led to a drastic improvement of the bounds on the mixings of the heavy quarks and the τ–lepton [76], that were otherwise poorly constrained [47]. The present accuracy leads to a general improvement of the limits on all the mixing angles, as we shall discuss in the result section.

i) Z decay widths

Eq. (2.22) is affected by mixing through the couplings $v_f = t_3^f\left[(c_L^f)^2 + (s_R^f)^2\right] - 2Q^f s^2_{eff}(f)$ and $a_f = t_3^f\left[(c_L^f)^2 - (s_R^f)^2\right]$ (see eqs. (3.10) and (2.23)), and by the factor G_F/G_μ, becoming

$$\Gamma_{Z\to f\bar{f}} = N_c^f \frac{M_Z}{12\pi}\sqrt{2}G_F M_Z^2 \rho_f (a_f^2 + v_f^2)(1+\delta^f_{QED})(1+\delta^f_{QCD}), \tag{4.14}$$

The value $\alpha_s(M_Z^2) = 0.118 \pm 0.008$, determined from jet analysis in hadronic Z decays [56], does not depend on fermion mixings, so it can be used safely for our purposes. We notice that mixings affect also the effective weak mixing angle of eq. (2.23), which becomes

$$s^2_{eff}(f) = \frac{1}{2}\left[1 - \sqrt{1 - \frac{G_\mu}{G_F}\frac{4A}{\rho M_Z^2}\left(\frac{1}{1-\Delta\alpha} + \Delta\bar{r}_f^{rem}\right)}\right]. \tag{4.15}$$

Hence, since G_μ/G_F enters the definition of the effective weak–mixing angle, all the LEP measurements contribute indirectly to bound the four mixings involved in the μ–decay.

Let us turn now to the asymmetries. Eq. (2.26) for the Forward–Backward asymmetries and eq. (2.27) for the τ polarization asymmetry are affected by mixings through the coplings v_f, a_f. We will consider first the leptonic and then the hadronic asymmetries.

ii) Leptonic asymmetries.

The combined measurement of the Z–widhts and of the FB–asymmetries allows for an independent determination of v_ℓ and a_ℓ, and turns out to be quite effective for constraining both the right and left mixing angles even in the "joint fits" where all the mixings are allowed to be present simultaneously.

The presence of mixing–induced RHC could in principle affect the experimental results for the τ polarization asymmetry quoted in chapter 2, but this effect is $O(s^4)$ and can thus be neglected.

iii) Heavy flavours

In our individual fits we have used the PEP/PETRA averages for a_b and a_c quoted in ref. [71]. In the joint analysis it is no more consistent to include these results since each axial coupling is determined while keeping the others fixed at their SM value, so in this case we have restricted our set of data by including only the c FB asymmetry measured with the D^*–tagging technique [73,72].

The measurements of the leptonic asymmetries in weak–electromagnetic interference do not improve significantly the constraints, and have not been included in our fit.

4.2 Results

To obtain the constraints on the mixing parameters s_i^2 we have confronted for each observable the theoretical expression X_α^{th}, worked out in section 1, with the corresponding experimental result $X_\alpha^{exp} \pm \sigma_\alpha$, given in chapter 2, by constructing a χ^2 function

$$\chi^2 = \sum_{\alpha,\beta} \frac{(X_\alpha^{th} - X_\alpha^{exp})}{\sigma_\alpha} (C^{-1})_{\alpha\beta} \frac{(X_\beta^{th} - X_\beta^{exp})}{\sigma_\beta} \tag{4.16}$$

where the C represents the matrix of correlations.

Some care must be paid in the interpretation of the confidence levels from the χ^2 since the variables s_i^2 are bounded in [0,1]. For each parameter we then assume a probability distribution

$$P(s_i^2) = N_i \ e^{-\chi^2(s_i^2)/2} \tag{4.17}$$

with $N_i^{-1} = \int_0^1 \exp(-\chi^2(s_i^2)/2) \ ds_i^2$. For the joint fits, in which all mixing parameters are allowed to vary simultaneously, the χ^2 function in the expression for $P(s_i^2)$ is minimized with respect to all the remaining parameters for each value of s_i^2.

The 90% c.l. upper bounds $\bar{s}_i^2$ are computed by requiring

$$\int_0^{\bar{s}_i^2} P(s_i^2) \ ds_i^2 = 0.90 \tag{4.18}$$

under the additional condition $\chi^2(\bar{s}_i^2) > \chi^2(0)$ that, if not satisfied, would be a signature for non–zero mixing angles at 90% c.l..

Although there are more than 20 mixing parameters, the large number of observables allows to constrain all of them. The inclusion of the recent results from LEP, together with the updated NC and CC results, have considerably improved almost all the previous limits [47,76]. Our results [31] for the 90 % c.l. bounds obtained in the individual and joint analyses are collected in table IV.

For simplicity we have assumed $\Lambda_e = \Lambda_\mu = \Lambda_\tau$ (corresponding to ordinary-exotic mixings of the same kind for the three neutrinos) but these parameters could in principle differ. In the individual analysis, since only the bounds on the neutrino mixings may depend on the value of Λ, we just show the results for $\Lambda = 2$. Furthermore, since the electron and muon neutrino mixings are mainly constrained by CC measurements, they are largely independent of the value of Λ. In contrast, for the τ neutrino different values of Λ led to different bounds, since in this case the LEP measurement of Γ_Z gives an important constraint. The *upper* bounds for ν_τ are respectively $(s_L^{\nu_\tau})^2 < 0.098, 0.032, 0.015$ for $\Lambda_\tau = 0, 2, 4$ corresponding to neutrino mixings with heavy ordinary doublets in sequential or vector doublets, with heavy singlets and with exotic doublets respectively. For the joint bounds, we present all the results for $\Lambda = 0$, 2 and 4.

One possibility that we have not considered for simplicity is the presence of *light* neutrinos that are mainly singlets. These could appear for instance in models where the light neutrinos are Dirac particles. These light singlets could mix with exotic doublets and hence couple to the Z, giving rise to a new invisible decay channel. The additional parameters s_R^ν describing these mixings would then be constrained by the measurement of Γ_Z. This would affect mainly the bounds on the τ neutrino mixings in the joint analysis (for $\Lambda_\tau \neq 0$), while the other bounds would essentially remain unmodified.

In the last column of table IV we list, for each mixing angle, the observables that are more important for establishing the constraints. Often a tight constraint set by some accurate measurements can be evaded in the joint analysis, since the deviations caused by the mixing under consideration may be canceled in these observables by adjusting other mixings to non–zero values. Other observables, for which the possibilities of cancellations are more restricted, can then become important in the determination of the joint bounds even if they were not decisive for the individual fits. In table IV these observables are labeled with a (*). This happens *e.g.* for Γ_Z and Γ_{had}, that are crucial for the single bounds but that should be supplemented by other constraints in the joint analyses since they depend on several mixing parameters. Hence, the large number of measurements at our disposal plays a crucial rôle for setting the limits.

A look at table IV makes apparent that the measurements of the Z partial and total widths contribute to the limits on all the exotic mixings. The bounds on the leptons and b–quark mixings receive further contributions from the on–resonance asymmetries, while PEP and PETRA off–resonance asymmetries help to strengthen the bounds for the c quark.

For the fermions of the first generation and for the μ_L and ν_L^μ leptons, both the 'low-energy' NC constraints (especially ν–q scattering and to a smaller extent the e–q sector) and the CC constraints on the unitarity of the CKM matrix are also important. These last quantities also bound the mixings $|V_{ui}|$ and $|V_{ci}|$ with sequential or vector doublets, as well as the parameters κ_{ij}, that are further constrained by direct searches of induced hadronic RHC's.

Due to the fact that the presence of the mixings modify the fermion couplings, the various determinations of the effective weak angle cannot be used as direct measurements. However since the theoretical expression for s_{eff} depends on the ratio G_F/G_μ, besides the direct constraints, the combination of all the LEP and NC experiments put also important indirect constraints to the mixings that appear in μ decay. These indirect bounds are quite effective for the electron and muon neutrino mixings, and are of some relevance also for $(s_L^\mu)^2$ in the joint analyses.

These two indirect sources of constraints have been denoted respectively with s_{eff}^{LEP} and s_{eff}^{NC} in table IV.

The W boson mass, that also constrains the ratio G_μ/G_F, is not very important in the individual analysis due to its present experimental error. However, it gains relevance in the joint fits since it does not allow for accidental cancellations between different mixings, as usually happens for LEP measurements.

For the left handed charged leptons and neutrinos, the constraints on lepton universality are also crucial. Some peculiarities arise in the $\tau - \nu_\tau$ sector, since to some extent the τ-decay measurements are better accounted for with non-universal CC lepton couplings (see e.g. ref. [40]). In particular, non–vanishing τ_L and/or ν_L^τ mixings weaken the $W\tau\nu_\tau$ coupling, allowing for a longer τ lifetime, as is favoured by experiments. The excellent agreement of the accurate LEP measurements with the SM predictions forces the overall probability distribution to be consistent with vanishing values for the τ and ν_τ mixings. However, if ν_τ mainly mixes with an ordinary sequential or vector doublet neutrino ($\Lambda_\tau \simeq 0$), the NC experiments are ineffective for constraining this mixing. In this case, both in the individual and in the joint analyses, we find that the value $s_L^{\nu_\tau} = 0$ falls out of the 90% confidence regions, that are respectively $0.0075 < s_L^{\nu_\tau} < 0.098$ and $0.0057 < s_L^{\nu_\tau} < 0.097$. However, within two standard deviations the data are consistent with zero mixing.

Another complication in the analysis is due to a peculiarity in the behaviour of the observables involving the d_R-type quark mixings. Indeed for $(s_R^q)^2 \simeq 0.3$ ($q = d,\ s,\ b$), the s^4 terms cancel against the quadratic ones inside both $v_q a_q$ and $v_q^2 + a_q^2$, that are the only combinations of couplings measurable at the Z–peak. Since the constraints on s_R^s and s_R^b are provided essentially by LEP experiments, the corresponding χ^2 distributions are characterized by two equivalent minima, one lying around vanishing value for the mixing and a second one near 0.3 and as a consequence the confidence intervals are split into two disjoint regions. Actually, due to the low central value of the b-quark axial–vector coupling as extracted from the asymmetries in the γ–Z interference region [71], the value $(s_R^b)^2 \simeq 0.3$ is even in slightly better agreement with the data. For the bounds in table IV we have conservatively integrated over both regions, however a restriction to the interval consistent with zero mixing gives $(s_R^s)^2 \lesssim 0.09$ and $(s_R^b)^2 \lesssim 0.10$, *i.e.* about three times tighter limits.

We can add a final comment about the interplay between the mixings and the bounds on the top mass. A fit to m_t leaving all the mixings free to vary, indicates that the preferred value is shifted downwards by about 25 GeV with respect to the case when all the mixings are set to zero. As already noted this is mainly due to the anticorrelation with the mixings that appear inside the ratio G_μ/G_F. As a consequence of the large number of free parameters the error is larger, and the upper bound on m_t is slightly relaxed. However, considering that also the loop effects of the new heavy fermions are expected to lower the upper bound on m_t, we can conclude that in general a 'light' top is preferred in models of this kind.

TABLE IV. 90 % c.l. upper bounds on the ordinary-exotic fermion mixings for the individual fits, where only one parameter is allowed to vary, and for the joint fits where cancellations between different mixings can occur. The observables that mainly contribute to determine the numerical values of the bounds are listed in the last column (those labeled by an asterisc (*) are effective only in the joint analyses). $s_{eff}^{\rm LEP}$ and $s_{eff}^{\rm NC}$ refer to the effective weak mixing angle, from Z–peak and NC experiments, which contribute indirectly to constrain the mixings in G_F/G_μ.

	Individual	Joint			Source
		$\Lambda=2$	$\Lambda=0$	$\Lambda=4$	
$(s_L^e)^2$	0.0047	0.015	0.0090	0.015	$\Gamma_e, M_W^*, A_\mu^{\rm FB*}, eq^*, g_e^*$
$(s_R^e)^2$	0.0062	0.010	0.0082	0.010	$\Gamma_e,\ A_e^{\rm FB},\ A_\mu^{\rm FB*},\ \nu e^*$
$(s_L^\mu)^2$	0.0017	0.0094	0.0090	0.011	$V_{ui}^2, \nu q, g_\mu, \Gamma_\mu, s_{eff}^{\rm LEP}{}^*, M_W^*$
$(s_R^\mu)^2$	0.0086	0.014	0.014	0.013	$\Gamma_\mu,\ A_\mu^{\rm FB}$
$(s_L^\tau)^2$	0.011	0.017	0.015	0.017	$\Gamma_\tau,\ A_\tau^{\rm FB}, g_\tau,\ A_\tau^{pol*}$
$(s_R^\tau)^2$	0.011	0.012	0.014	0.012	$\Gamma_\tau,\ A_\tau^{pol}, A_\tau^{FB},\ g_\tau^*$
$(s_L^u)^2$	0.0045	0.019	0.015	0.019	$V_{ui}^2,\ \Gamma_h,\ \Gamma_Z, eq, \nu q$
$(s_R^u)^2$	0.018	0.024	0.025	0.024	$\nu q,\ \Gamma_h,\ \Gamma_Z,\ eq$
$(s_L^d)^2$	0.0046	0.019	0.016	0.019	$V_{ui}^2,\ \Gamma_h,\ \Gamma_Z,\ \nu q$
$(s_R^d)^2$	0.020	0.030	0.028	0.029	$eq,\ \Gamma_h,\ \Gamma_Z,\ \nu q$
$(s_L^s)^2$	0.011	0.038	0.039	0.041	$\Gamma_h,\ \Gamma_Z,\ V_{ui}^2$
$(s_R^s)^2\,\dagger$	0.36	0.67	0.63	0.74	$\Gamma_h,\ \Gamma_Z$
$(s_L^c)^2$	0.013	0.040	0.042	0.042	$\Gamma_h,\ \Gamma_Z,\ \Gamma_c^*,\ A_c^{\gamma Z*}$
$(s_R^c)^2$	0.029	0.097	0.10	0.099	$\Gamma_h, \Gamma_Z, A_c^{\gamma Z*}, \Gamma_c^*, A_c^{\rm FB*}$
$(s_L^b)^2$	0.011	0.070	0.072	0.069	$\Gamma_h,\ \Gamma_Z,\ \Gamma_b,\ A_b^{\rm FB*}$
$(s_R^b)^2\,\dagger$	0.33	0.39	0.40	0.39	$\Gamma_b,\ \Gamma_Z, \Gamma_h,\ A_b^{\gamma Z},\ A_b^{\rm FB*}$
$(s_L^{\nu_e})^2$	0.0097	0.015	0.016	0.014	$s_{eff}^{\rm LEP}, g_e, s_{eff}^{\rm NC}, M_W^*$
$(s_L^{\nu_\mu})^2$	0.0019	0.015	0.0087	0.011	$V_{ui}^2, g_\mu, \nu q, s_{eff}^{\rm LEP}, M_W^*$
$(s_L^{\nu_\tau})^2\,\dagger$	0.032	0.064	0.097	0.035	$\Gamma_Z,\ g_\tau$
$\sum_{i=4}^n K_{ui}^2$	0.0048	0.014	0.010	0.018	V_{ui}^2
$\lvert\kappa_{ud}\rvert$	0.0011	0.0059	0.0060	0.0058	V_{ui}^2, νq, RHC's, νe^*
$\lvert\kappa_{us}\rvert$	0.0054	0.0061	0.0061	0.0061	V_{ui}^2, RHC's
$\sum_{i=4}^n K_{ci}^2$	0.53	0.76	0.76	0.76	V_{ci}^2
$\lvert\kappa_{cd}\rvert$	0.31	0.31	0.31	0.31	RHC's
$\lvert\kappa_{cs}\rvert$	0.24	0.29	0.29	0.29	V_{ci}^2, RHC's

† For some peculiarities that occur for s_R^s and s_R^b, and for a discussion of the bounds on $s_L^{\nu_\tau}$, see text.

4.3 Conclusions

As a summary, we have analysed the limits on the mixings of the known leptons and quarks with possible heavy fermions with exotic $SU(2)_L$ assignments. We have obtained significant constraints on a very large set of mixing parameters by performing a detailed global analysis of the available electroweak data.

In order to guarantee the experimentally observed absence of FCNC, we have assumed that each ordinary charged fermion mixes with a unique exotic state, in which case just one mixing angle per degree of freedom is enough to describe the effects of the mixing. For the neutrinos there is no experimental evidence of FCNC suppression, but since one has to sum over the flavor of the unobserved final ν states, again just one mixing angle per neutrino flavor allows to describe the mixings, with the addition of an effective parameter (Λ) that takes into account the type of exotic neutrinos involved.

In order to constrain the mixing angles we have analyzed the effects that they could induce in the couplings between the light fermions and the weak bosons. Very accurate measurements of the fermion weak–couplings are provided by several experiments, as for example tests on CC universality and on the unitarity of the CKM matrix, limits on induced right-handed currents, collider measurements of M_W, low-energy NC experiments (ν-scattering, atomic parity violation and polarized $e - D$ scattering) and in particular the huge amount of data obtained at LEP and SLC from experiments at the Z-resonance. The results of our analysis are collected in table IV.

If only one mixing angle is considered at a time, for most of the mixing factors $(s^f)^2$ the limits are below the 1 % level, with the exception of the mixings of

u_R, d_R, c_R and $\nu_{\tau L}$ that are of the order of a few percent and those of s_R and b_R that are still poorly constrained to values $\lesssim 1/3$. Allowing for accidental cancellations among different mixings the constraints are relaxed by a factor between 2 and 5.

Acknowledgements

I would like to thank my supervisor Antonio Masiero for the physics he taught me, and for his friendly, nice and tolerant guidance in more than one year of my studies.

The main part of this thesis arises from exciting collaborations with my friends Enrico Nardi and Esteban Roulet. Enrico, who has been my office fellow for four years, has been teaching me particle physics since the time of the first year examinations; Esteban has been guiding me since the second year, when I was preparing my Master thesis. They have organized a large part of my research, and made the work enjoyable with their warm, fascinating company.

Another part of the thesis arises from a collaboration with Riccardo Barbieri, who greatly influenced me even through such a short direct contact, Antonio, and M.M. Guzzo.

Since this is my last thesis, I thank here all the persons who have taught me physics and helped me in these years, in particular my first supervisors Beppe Bandelloni, who introduced me in the world of research, and Graciela Gelmini.

I am grateful to Pasquale Pavone for his continuous, precious help in solving all kinds of computer problems, and to him and to Kurt for being always close to me in these four years at the SISSA. Here I have lived a unique period with the nice and friendly atmosphere and the particular 'SISSA' way to be together, and especially for all the extraordinary friends I have found. My thanks go to all of them, in particular to the above ones and to Alfio, Annarita, Elena, Fabio, Marian, and Virginia. The SISSA club also played an important role thanks to its organizers, above all Gregorio Falqui, Roberto Iengo, Guido Magnano (who taught me how to correctly tie my shoes, and helped me to sing like a bird, or 'a raven' as he would say), and, last but not least, Giuseppe Mussardo.

Bibliography

[1] C.S. Aulakh and R.N. Mohapatra, Phys. Rev. D119 (1983) 136; F. Zwirner, Phys. Lett. B132 (1983) 103; L.J. Hall and M. Suzuki, Nucl. Phys. B231 (1984) 419; I.H. Lee, Nucl. Phys. B246 (1984) 120; G.G. Ross and J.W.F. Valle, Phys. Lett. B151 (1985) 375; J. Ellis et al., Phys. Lett. B150 (1985) 142; S. Dawson Nucl. Phys. B261 297; R. Barbieri and A. Masiero, Nucl. Phys. B267 (1986) 679; R.N. Mohapatra, Phys. Rev. D11 (1986) 3457; V. Barger, G. Giudice and T.Y. Han, Phys. Rev. D40 (1989) 2987; E. Ma and P. Roy Phys. Rev. D41 (1990) 988; E. Ma and D. Ng Phys. Rev. D41 (1990) 1005; S. Dimopoulos, R. Esmailzadeh, L.J. Hall, J.P. Merlo, G.D. Sparkman, Phys. Rev. D41 (1990) 2099; L.H. Hall, Mod. Phys. Lett. A5 (1990) 467.

[2] R. Barbieri, M.M. Guzzo, A. Masiero and D. Tommasini, Phys. Lett. B252 (1990) 251.

[3] R. Barbieri and G. Fiorentini, Nucl. Phys. B304 (1988) 909.

[4] D.W. Sciama, preprint SISSA 29 A (1990).

[5] D.W. Sciama, preprint SISSA 28 A (1990).

[6] For a review, see H.P. Nilles, Physics Reports, 110 (1984) 1, and references therein.

[7] F. Zwirner, Phys. Lett. B132 (1983) 103;
R. Barbieri and A. Masiero, Nucl. Phys. B267 (1986) 679;
G.G. Ross and J.W.F. Valle, Phys. Lett. B151 (1985) 375;

J. Ellis, G. Gelmini, C. Jarlskog, G.G. Ross and J.W.F. Valle, Phys. Lett. B150 (1985) 142;
F. Gabbiani and A. Masiero, Nucl. Phys. B259 (1991) 323.

[8] V. Barger et al. in ref. [1].

[9] K.S. Babu and R.N. Mohapatra, Phys. Rev. Lett.64 (1990) 1705.

[10] W.S. Marciano and A. Sanda, Phys. Lett. B77 (1977) 303; B.W. Lee and R. Shrock, Phys. Rev. D60 (1977) 444; S. Petcov, Sov. J. Nucl. Phys. 25 (1977) 340; (E): Sov. J. Nucl. Phys. 25 (1977) 698; K Fujikawa and R. Shrock, Phys. Rev. Lett.45 (1980) 963.

[11] M. Voloshin, Yad. Fiz. 48 (1988) 804 [Sov. J. Nucl. Phys. 48 (1988) 512]; R. Barbieri and R. N. Mohapatra, Phys. Lett. B218 (1989) 225; T. Liu, Phys. Lett. B225 (1989) 148; K.S. Babu and R.N. Mohapatra, Phys. Rev. Lett.63 (1989) 228; G. Ecker, W. Grimus and H. Neufeld, Phys. Lett. B232 (1989) 217; D. Chang, W. Keung and G. Senjanovic, Phys. Rev. D42 (1990) 1599; M.I. Vysotsky, ICTP preprint IC/90/78 (1990).

[12] M. Leurer and N. Marcus, Phys. Lett. B237 (1990) 81.

[13] K.S. Babu and R.N. Mohapatra, Phys. Rev. D42 (1990) 3778.

[14] A. De Rújula and S.L. Glashow, Phys. Rev. Lett.45 (1980) 942.

[15] A.L. Mellot and D.W. Sciama, Phys. Rev. Lett.46 (1981) 1369.

[16] S. Tremaine and J.E. Gunn, Phys. Rev. Lett.42 (1979) 407; D.W. Sciama, preprint SISSA 31 A (1990).

[17] A. Zee, Phys. Lett. B93 (1980) 389; S. Petcov, Phys. Lett. B115 (1982) 401; R.N. Mohapatra, Phys. Lett. B201 (1988) 517; J.P. Ralston, D.W. McKay and A.L. Mellot, Phys. Lett. B202 (1988) 40.

[18] F. Gabbiani, A. Masiero and D.W. Sciama, Phys. Lett. B259 (1991) 323.

[19] E. Roulet and D. Tommasini, Phys. Lett. B256 (1991) 218.

[20] J. Maalampi and M. Roos, HU–TFT–91–10 (1991).

[21] K. Enqvist, A. Masiero and A. Riotto, in preparation.

[22] See for instance L. Wolfenstein, Phys. Lett. B107 (1981) 77; B. Kayser and A.S. Goldhaber, Phys. Rev. D28 (1983) 2341; B. Kayser, Phys. Rev. D30 (1984) 1023; S.M. Bilenky and S.T. Petcov, Rev. Mod. Phys. 59 (1987) 671.

[23] Rev. of Part. Prop., Phys. Lett. B239 (1990) 1.

[24] E. Roulet, Phys. Rev. D44 (1991) R953.

[25] M.M. Guzzo, A. Masiero and S. Petcov, Phys. Lett. B260 (1991)154;
V. Barger, R.J.N. Phillips and K. Wishnant, MAD/PH/648 (1991).

[26] E. Roulet, FERMILAB–PUB–91/206–A

[27] B.A. Campbell, S. Davidson, J. Ellis and K. Olive, Phys. Lett. B256 (1991) 457;
W. Fishler, G.F. Giudice, R.G. Leigh and S. Paban, Phys. Lett. B258 (1991) 45.

[28] A. Masiero, DFPD 91/TH/11.
[29] A. Masiero and J.W.F. Valle, Phys. Lett. B251 (1990) 273.
[30] M. Voloshin, M. Vysotskii and L.B. Okun, JETP 64 (1986) 446; Sov. J. Nucl. Phys. 44 (1986) 440.
[31] E. Nardi, E. Roulet and D. Tommasini, SISSA 104/91/EP (FERMILAB 91/207-A), submitted to Nucl. Phys. B.
[32] F. Jegerlehner, PSI–PR–89–23 (1989); PSI–PR–91–08;16 (1991).
[33] ALEPH Collaboration, D. Decamp et al., CERN–PPE/91–105;
DELPHI Collaboration, P. Abreu et al., CERN–PPE/91–95;
L3 Collaboration, B. Adeva et al., L3 Prep. # 028 (1991);
OPAL Collaboration, M. Alexander et al., CERN–PPE/91–81.
[34] A. Sirlin, Phys. Rev. D22 (1980) 971; Phys. Rev. D29 (1984) 89;
W. J. Marciano and A. Sirlin, Phys. Rev. D29 (1984) 945.
[35] M. Veltman, Nucl.Phys. B 123 (1977) 89;
M.B. Einhorn, D.R.T. Jones, M. Veltman, Nucl.Phys. B 191 (1981) 146.
[36] M. Consoli and W. Hollik, 'Z physics at LEP 1' vol. 1, eds. G. Altarelli et al., CERN 89–08;
G. Burgers and F. Jegerlehner, ibidem;
W. Hollik, CERN–TH.5661/90 (FEB. 1990);
G. Burgers and W. Hollik, in 'Polarization at LEP' vol. 1, eds. G. Alexander et al., CERN 88–06;
B. W. Lynn, M. E. Peskin and R. G. Stuart, in 'Physics at LEP' vol. 1, eds. J. Ellis and R. Peccei CERN 86-02 (1986);
D.C. Kennedy and B.W. Lynn, Nucl. Phys. B 322 (1989) 1;
J.G. Im, D.C. Kennedy, B.W. Lynn and R.G. Stuart, Nucl. Phys. B 321 (1989) 83;
J.L. Rosner, EFI 90–18 (June 1990).
[37] UA2 Collaboration, J. Alitti et al., Phys. Lett. B241 (1990) 150;
CDF Collaboration, F. Abe et al., Phys. Rev. Lett.65 (1990) 2243.
[38] UA1 Collaboration, C. Albajar et al., Phys. Lett. B185 (1987) 233;
UA2 Collaboration, J. Alitti et al., CERN–PPE/91–69.
[39] L3 Collaboration, B. Adeva et al., L3 Prep. # 031 (1991);
OPAL Collaboration, G. Alexander et al., in ref. [63].
[40] Xue-Quian Li and Tao Zhi-jian, Phys. Rev. D43 (1991) 3691.
[41] T.N.Truong, Phys. Rev. D30 (1984) 1509;
F.J. Gilman and S.H. Rhie, Phys. Rev. D31 (1985) 1066;
F.J. Gilman, Phys. Rev. D35 (1987) 3541.
[42] W. J. Marciano, BNL–45999 (1991).
[43] W. Jaus and G. Rasche, Phys. Rev. D41 (1990) 166;
D. H. Wilkinson, TRI–PP–90–44 (1990); Phys. Lett. B241 (1990) 317.

[44] A. Sirlin, CU–TP–505 (1990);
D. G. Hitlin, CALT–68–1722 (1991).

[45] CDHS Collaboration, Abramowicz et al. Z. Phys. C12 (1982) 225; Z. Phys. C15 (1982) 19.

[46] J. F. Donoghue and B. R. Holstein, Phys. Lett. B113 (1982) 382.

[47] P. Langacker and D. London, Phys. Rev. D38 (1988) 886.

[48] P. Langacker and D. London, Phys. Rev. D39 (1989) 266.

[49] P. Langacker and D. London, Phys. Rev. D38 (1988) 907.

[50] CHARM-II Collaboration, D. Geiregat et al., Phys. Lett. B259 (1991) 499.

[51] CHARM Collaboration, J. Dorenbosch et al., Z. Phys. C41 (1989) 567.

[52] BNL collaboration, K. Abe et al., Phys. Rev. Lett.62 (1989) 1709.

[53] S.A. Blundell, W.R. Johnson and J. Sapirstein, Phys. Rev. Lett.65 (1990) 1411.

[54] M.C. Noecker, B.P. Masterson and C.E. Wieman, Phys. Rev. Lett.61 (1988) 310.

[55] C.Y. Prescott et. al., Phys. Lett. B77 (1978) 347; Phys. Lett. B84 (1979) 524.

[56] S. Bethke, CERN–PPE/91–36, and references therein.

[57] A.A. Akhundov, D. Bardin and T. Riemann; Nucl. Phys. B 276 (1988) 1;
F. Diakonos and W. Wetzel, HD–THEP–88-21 (1988);
W.Beenakker and W.Hollik, Z. Phys. C40 (1988) 141;
B.W. Lynn and R.G. Stuart, Phys.Lett. 252 B (1990) 676.

[58] E. Fernandez, CERN–PPE/90–151;
F. Dydak, CERN–PPE/91–14;
H. Burkhardt and J. Steinberger, CERN–PPE/91–50.

[59] OPAL Collaboration, M. Akrawy et al., Z. Phys. C50 (1991) 373.

[60] J.H. Kuhn, et al., in 'Z physics at LEP 1', vol. 1 eds. G. Altarelli et al., CERN 89–08;
J.H. Kuhn, et al., MPI-PAE/PTh-49/89 (Aug 1989).

[61] D. Bardin et al., Phys. Lett. B229 (1989) 405;
M. Böhm et al., CERN–TH–5536/89 (1989);
Z. Was and S. Jadach, Phys. Rev. D41 (1990) 1425;
D. Bardin et al., Nucl. Phys. B351 (1991) 1;
D. Bardin et al., Phys. Lett. B255 (1991) 290;
S. Jadach, M. Skrzypek and B. F. L. Ward, Phys. Lett. B257 (1991) 173;
S. Jadach, B. F. L. Ward and Z. Was, Phys. Lett. B257 (1991) 213;
A. A. Akhundov, D. Y. Bardin and A. Leike, Phys. Lett. B261 (1991) 321.

[62] S. Jadach and Z. Was, in 'Z physics at LEP 1', vol. 1 eds. G. Altarelli et al., CERN 89–08; and Phys. Lett. B219 (1989) 103;

B.C. Barish and R. Stroynowsky, Physics Reports, 157 (1988) 1;
M. Perl, SLAC–PUB-4739, (1988).

[63] ALEPH Collaboration, D. Decamp et al., CERN–PPE/91–94;
OPAL Collaboration, G. Alexander et al., CERN–PPE/91–103.

[64] L3 Collaboration, B. Adeva et al., Phys. Lett. B261 (1991) 177;
OPAL Collaboration, M. Akrawy et al., Phys. Lett. B263 (1991) 311;
ALEPH Collaboration, D. Decamp et al., Phys. Lett. B244 (1990) 551;
DELPHI Collaboration, P. Abreu et al., CERN–PPE/90–118;
MARK II Collaboration, J.F. Kral et al., Phys. Rev. Lett.64 (1990) 1211;

[65] L3 Collaboration, B. Adeva et al., in ref. [64].

[66] ALEPH Collaboration, in ref [64];
OPAL Collaboration, M. Akrawy et al., in ref. [64];
DELPHI Collaboration, P. Abreu et al., Phys. Lett. B252 (1990) 140;
OPAL Collaboration, M. Akrawy et al., Phys. Lett. B262 (1991) 341.

[67] ALEPH Collaboration, D. Decamp et al., Phys. Lett. B263 (1991) 325;
L3 Collaboration, B. Adeva et al., Phys. Lett. B252 (1990) 713;
OPAL Collaboration, M. Akrawy et al., in ref. [64].

[68] I.Bigi, Phys.Lett. 155 B (1985) 125;
A.Djouadi, J.H.Kühn and P.M.Zerwas, Z. Phys. C46 (1990) 411.

[69] L3 Collaboration, B. Adeva et al., Phys. Lett. B252 (1990) 703;
ALEPH Collaboration, D. Decamp et al., Phys. Lett. B258 (1991) 236;
UA1 Collaboration, C. Albajar et al., Phys. Lett. B262 (1991) 171.

[70] ARGUS Collaboration, H. Albrecht et al., Phys. Lett. B192 (1987) 254;
CLEO Collaboration, M. Artuso et al., Phys. Rev. Lett.252 (1990) 703.

[71] CELLO Collaboration, H.J. Behrend et al., Z. Phys. C47 (1990) 333.

[72] JADE Collaboration, E. Elsen et al., Z. Phys. C46 (1990) 349.

[73] JADE Collaboration, F. Ould-Saada et al., Z. Phys. C44 (1989) 567.

[74] J. Ellis and G.L. Fogli, Phys. Lett. B 213 (1988) 526;
J. Ellis and G.L. Fogli, Phys. Lett. B 232 (1989) 139;
A. Blondel, CERN–EP/90–10, (January 90);
J. Ellis and G.L. Fogli, Phys. Lett. B 249 (1990) 543.

[75] J. Maalampi and M. Roos, Phys. Rep. 186 (1990) 53.

[76] E. Nardi and E. Roulet, Phys. Lett. B248 (1990) 139.

[77] U. Amaldi et al., Phys.Rev. D 36 (1987) 1385.

[78] G. Costa et al., Nucl. Phys. B297 (1988) 244.

[79] C. Foudas et al., Phys. Rev. Lett.64 (1990) 1207.

[80] J. Ellis and G.F. Fogli, Phys. Lett. B249 (1990) 543;
P. Langacker, UPR–0435T (Aug 1990).

[81] J. Layssac, F.M. Renard and C. Verzegnassi, LAPP-TH-290-90-REV. (1991);
M.C. Gonzalez García and J.W.F. Valle; Phys. Lett. B259 (1991) 365;

G. Altarelli et al., CERN–TH-6051/91;
P. Langacker and M. Luo, UPR-0476T (1991);
F. del Aguila, J.M. Moreno and M. Quirós, Phys. Rev. D41 (1990) 134; err. ibid. 42 (1990) 262; Phys. Lett. B254 (1991) 497.

[82] M.E. Peskin and T. Takeuchi Phys. Rev. Lett.65 (1990) 964;
D.C. Kennedy and P. Langacker Phys. Rev. Lett.65 (1990) 2967; E: ibid 66 (1991) 395; UPR-0467T (Mar. 1991);
W.J. Marciano and J.L. Rosner, Phys. Rev. Lett. 65 (1990) 2963;
G. Altarelli and R. Barbieri, Phys. Lett. B253 (1991) 161.

[83] J. Maalampi, K. Mursula and M. Roos, Nucl. Phys. B207 (1982) 233;
J. Maalampi and K. Mursula, Z. Phys. C16 (1982) 83; Nucl. Phys. B269 (1986) 109;
K. Enqvist, K. Mursula and M. Roos, Nucl. Phys. B226 (1983) 121;
K. Enqvist, J. Maalampi and M. Roos, Phys. Lett. B176 (1986) 396;
T. Rizzo, Phys. Rev. D34 (1986) 2076; Phys. Rev. D34 (1986) 2163;
P. M. Fishbane, R. E. Norton and M. J. Rivard, Phys. Rev. D33 (1986) 2632;
V. Barger, R. J. Phillips and K. Whisnant Phys. Rev. Lett.57 (1986) 48;
M. Gronau, C. N. Leung and L. Rosner, Phys. Rev. D29 (1984) 2539.

[84] P. Langacker, M. Luo and A.K. Mann, UPR-458T (1991).

[85] for a review, see J.L. Hewett and T.G. Rizzo, Phys. Rep. 183 (1989) 195.